USER GROUPING IN WIRELESS NETWORKS WITH FULL DUPLEX BASE STATIONS AND LEGACY MOBILE STATIONS

A THESIS SUBMITTED TO

THE GRADUATE SCHOOL OF ENGINEERING AND SCIENCE

OF BILKENT UNIVERSITY

IN PARTIAL FULFILLMENT OF THE REQUIREMENTS FOR

THE DEGREE OF

MASTER OF SCIENCE

IN

ELECTRICAL AND ELECTRONICS ENGINEERING

By

Deniz Ünal

August 2018

User Grouping in Wireless Networks with Full Duplex Base Stations and Legacy Mobile Stations
By Deniz Ünal
August 2018

We certify that we have read this thesis and that in our opinion it is fully adequate, in scope and in quality, as a thesis for the degree of Master of Science.

Ezhan Karaşan(Advisor)

Nail Akar

Murat Alanyalı

Approved for the Graduate School of Engineering and Science:

Ezhan Karaşan
Director of the Graduate School

ABSTRACT

USER GROUPING IN WIRELESS NETWORKS WITH FULL DUPLEX BASE STATIONS AND LEGACY MOBILE STATIONS

Deniz Ünal
M.S. in Electrical and Electronics Engineering
Advisor: Ezhan Karaşan
August 2018

Improving spectral efficiency is a key objective in next generation wireless networks. Recent advances in self-interference cancellation techniques made in-band full-duplex wireless communications possible. Unlike half-duplex systems which require orthogonal frequency or time resources to separate transmission and reception, in-band full-duplex radios utilize the channel bidirectionally and theoretically can double the ergodic capacity. However due to cost, power consumption and complexity constraints, mobile stations may not support this technology. In this work, operation of full-duplex base stations with legacy half-duplex mobile stations is considered. An inherent issue of this topology is the presence of significant inter-user interference between half-duplex mobile stations. In order to manage this at network level, an optimization problem is formulated for a cellular network topology. Solution methods and their corresponding sum throughput are compared with respect to the number of mobile stations. An analytic solution is presented to evaluate the throughput and full-duplex gains of random pairing method for the same scenario. Then the case of limited channel state information is evaluated and a learning strategy is introduced to extend the user pairing problem to a continuous case. Performance evaluation with 100 mobile stations show that the proposed learning strategy can reduce the overhead airtime more than 80%. A weighted random sequential algorithm which is integrated to the learning process is proposed, and its performance evaluation under random walk and random waypoint mobility cases are performed.

Keywords: Wireless Networks, Full-Duplex, Mobility, Station Pairing.

ÖZET

TAM ÇİFT YÖNLÜ BAZ İSTASYONLU VE ESKI MOBİL İSTASYONLU KABLOSUZ AĞLARDA KULLANICI GRUPLAMASI

Deniz Ünal
Elektrik Elektronik Mühendisliği, Yüksek Lisans
Tez Danışmanı: Ezhan Karaşan
Ağustos 2018

Spektral verimliliği arttırmak yeni nesil kablosuz ağların önemli hedeflerinden biridir. Yeni öz-girişim giderim yöntemleriyle ilgili son gelişmeler aynı bant tam çift yönlü kablosuz iletişimi olası hale getirmiştir. Aynı bant çift yönlü kablosuz radyolar verici ve alıcı ayırması için dikey frekans ya da zaman kaynağı gerektirmediğinden çift yönlü sistemlere göre kuramsal olarak ergodik kapasiteyi iki katına çıkarabilir. Öte yandan maliyet, güç tüketimi ve karmaşıklık kısıtlamaları nedeniyle mobil istasyonlar bu teknolojiyi kullanmayabilir. Bu çalışmada tam çift yönlü baz istasyonları ve eski çift yönlü mobil istasyonlarının çalışması ele alınmıştır. Bu topolojinin doğal bir sorunu çift yönlü mobil istasyonlar arasındaki kullanıcı arası girişimdir. Bunu ağ seviyesinde yönetmek için küçük hücre ağları için bir optimizasyon problemi formülleştirilmiştir. Çözüm yöntemleri ve bunların toplam çıktıları kullanıcı sayısı da dikkate alınarak karşılaştırılmıştır. Rastgele eşleme yönteminin çıktısını ve tam çift yönlü kazançlarını değerlendirmek için analitik bir çözüm sunulmuştur. Daha sonra sınırlı kanal durum bilgisi senaryosu değerlendirilmiş ve bir öğrenme stratejisi ortaya konularak kullanıcı eşleme problemi genişletilmiş bir hücrede sürekli hale getirilmiştir. 100 mobil istasyon ile yapılan hesaplamalar öğrenme stratejisinin yayın süresi yükünü %80'den fazla azaltabildiği görüşmüştür. Öğrenme stratejisiyle birleştirilmiş bir ağırlıklı sıralı rastgele algoritma önerilmiş ve performansı rastgele yürüyüş ve rastgele güzergah hareketlilik modelleriyle değerlendirilmiştir.

Anahtar sözcükler: Kablosuz Ağlar, Tam çift yönlü, Hareketlilik, İstasyon Eşleme.

Acknowledgement

First and foremost, I would like to thank my advisor Prof. Ezhan Karaşan for his guidance, encouragement, helpful advice, and patience.

I also thank to Prof. Nail Akar and Prof. Murat Alanyalı their valuable contributions to my thesis committee and examining my thesis.

Finally, for their continuous support during my studies I am grateful to all my friends and family.

Contents

List of Figures

List of Tables

Chapter 1

Introduction

The demand for mobile data traffic is growing at a massive rate. A recent report by Cisco states that mobile data traffic has increased 18-fold over from 2011 to 2016. Their forecast includes a 49% annual compounding increase in mobile data which is projected to reach 49 exabytes by 2021 [1].

With the emerging applications such as virtual reality, augmented reality, mobile cloud services, and streaming services the need for wireless networks that support larger capacity can only increase. International Telecommunications Union (ITU) acknowledges the growth in mobile communications and include improving spectral efficiency for next generation wireless networks in their roadmap [2].

Textbooks on wireless communication often state using the same channel for transmission and reception is not possible in multi user systems. In his book Wireless Networks, Molisch refers the issue "transmit and receive levels of wireless signals are so different that the transmitted signal would "swamp" the RX and make it impossible to detect the receive signal" [3]. Envisioned communication scheme which is referred in this context is called full-duplex.

Traditional approach to this problem involves orthogonal resources in frequency, time, or spatial domains. In frequency division duplexing (FDD) different carrier frequencies are assigned for transmission and reception by extending

resources on frequency spectrum. In time division duplexing (TDD) transmit and receive are done consecutively through the same channel in which devices continuously switch their operating modes. In addition to duplexing techniques directional transmission methods can be utilized. This is practically achieved via a set of antenna elements to prevent signals in two different directions from interfering with each other by segregating their propagation regions.

Fundamental obstacle against simultaneous two way operation is self-interference (SI) effect. Self interference is essentially the signal originated from transmitter which is fed back to receiver of the same device. It is expected to have several orders of magnitude larger power than received signal in practical systems e.g. 90-100 dB. SI not only saturates the sampling circuit of the receiver chain but also conceals received signal as it is additive.

Self interference can be decomposed into two sources as direct and reflected paths [4]. In transceivers with single antenna, direct SI is caused by the leakage in circulator component from transmit port to receive port. Systems with separate antennas on the other hand encounter direct SI in the form of line-of-sight (LOS) effect from transmit antenna to receive antenna. Reflected SI is caused by non-line-of-sight (NLOS) components of the transmission that return back to the receiver. Direct path is the prominent component of SI as it is much more powerful than the latter one [5]. On the other hand, while direct SI mostly arises from transceiver architecture and can be characterized relatively conveniently, reflected SI is influenced by channel conditions and it is not straightforward to predict.

To enable full-duplex communication, self-interference cancellation technologies can be used to subtract SI component from the received signal. As a widely studied problem, such technologies tackle with conventional transceiver architectures at different blocks. Propagation domain approaches include separation of transmit and receive antennas to leverage path loss, using directional antennas, placement and cross-polarization arrangements for antennas [6, 7]. For the case of single antenna, duplexer circuits are used to provide isolation for direct SI. Analog domain technologies subtract the expected SI from received signal. While the basic implementations account for gain, phase and delay due to direct SI, adaptive

designs provide reconfiguration capabilities that allow tuning parameters to account for reflected SI components [8]. Digital domain technologies are employed after the received signal is sampled using the ADC. Surviving self interference is estimated and subtracted from the signal with DSP algorithms.

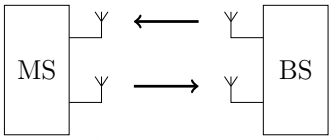

Figure 1.1: Bidirectional full-duplex

While SI cancellation techniques by themselves are not enough in real world environments, full-duplex breakthrough emerged when propagation, analog, and digital domain techniques are combined. Sufficient SI mitigation levels allow reliable full-duplex wireless communication. Demonstrations with experimental setups are reported [8, 9, 10], and research that consider small cell networks are reported in [11, 12]. Throughout the thesis unless noted otherwise we implicitly refer to in-band full-duplex when we use the term full-duplex.

Full-duplex wireless communication systems have the following advantages [4]:

- A perfect in-band full-duplex system can theoretically achieve twice the ergodic capacity of a half-duplex system.
- It provides some flexibility in spectrum management, as the resource allocation can be reconsidered to account for the choice of FD/HD mode for a given configuration.
- It can reduce the delay of feedback signals such as acknowledgment, repeat requests, control signaling. Since nodes do not have to wait for their turn they can track channel condition and control throughput better as well as provide support for rapid reconfiguration.
- SI cancellation can enhance network secrecy. While transmitted signal is subtracted from received signal at nodes communicating with each other, eavesdroppers can only capture the combination of two transmitted signals through medium of propagation.

- In the relay topology, it allows simultaneous transmission significantly reduce end to end delay.

Motivation on researching full-duplex networks can be justified with the fact that these benefits intersect with spectrum, latency and privacy demands of next generation wireless networks.

Performance limitations of the system is mainly due to imperfect SI cancellation, and a study on asymptotic behavior of capacity argues that the two fold increase in capacity is not possible if proper management is not in use [13].

Switching from network to user equipment perspective of the bidirectional full-duplex we observe some challenges. It is anticipated that additional analog circuitry for SI suppression to increase overall power consumption of mobile stations [14, 5]. Further advancements are needed to ensure compliance to energy efficiency objectives of next generation networks. Antenna design also poses spatial limitations. Dimensions for antenna such as presented in [15] require slightly more area than typical antennas used in contemporary mobile equipment. Passive isolation to limit electromagnetic coupling imposes requirements for relative spacing and positioning of antennas. Transmit and receive antennas needs to be separated by tens of centimeters and relative placement of these are critical which imposes mechanical design issues.

Contemporary mobile devices have tight design specifications on their sizing and battery life. Effectiveness of SI cancellation is influenced from these design parameters and originate a trade-off against performance [5]. Resulting compactness and energy efficiency concerns do not seem to be compatible with current state of the art SI cancellation subsystems.

It is not uncanny to foresee a progression course in which infrastructure needs to support coexistence of full-duplex base stations with legacy mobile stations which operate in half-duplex. This configuration is also widely anticipated in the literature and studied under various names such as base station topology, node-node topology, or full duplex on cell level.

In this topology, base station is connected to two different mobile stations, receiving packets from one and transmitting to another one. Information flowing in both directions represent separate logical channels. Mobile stations assume separate half-duplex operation and two links are not correlated with each other.

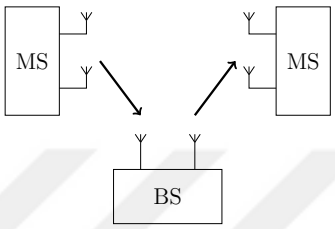

Figure 1.2: Full-duplex base station topology

Operation with legacy mobile stations extends the issues beyond bidirectional topology. In addition to SI cancellation problem discussed previously, receiving users are exposed to inter-user interference originated from transmitting user in this configuration. Receiving station has no prior information about neither of the two concurrent transmissions, and it is not capable of rejecting the interfering stream originated from transmitting station destined to base station.

In this configuration, presence of inter-user interference cannot be eradicated. Moreover depending on its intensity, it can render signal transmitted from base station obscure which reduces spectrum efficiency gains from using full-duplex. Unlike SI, this interference component is highly dependent on relative positioning of interfering and victim mobile stations. Considering a topology with several nodes at arbitrary locations, the interference level they experience can be regulated by controlling network resources they use. Interference management problem in this context can utilize scheduling users in pairs or adjusting their power levels.

In this thesis, we investigate the user grouping problem in wireless networks with full-duplex base stations and legacy mobile stations in dynamic environments with user mobility. Under mobility, user pairing problem needs to be constantly updated using the information retrieved from the network. To construct the problem we first establish and analyze user grouping in stationary scenarios, then we extend the problem in which channel state information needs to be

learned through reports from nodes. Finally we present heuristic algorithms for continuous complementary operation for pairing.

The thesis is organized as follows. In Chapter 2, a literature review on full-duplex wireless communications is provided. In Chapter 3, user pairing problem is introduced along with various solution methods and their performance figures are presented. In order to understand the dynamics of full-duplex cell with half-duplex users in an unsupervised setting, an analytic approach is employed with random pairing in Chapter 4. In Chapter 5, user pairing problem is transformed into a time variant framework. The process of learning network parameters to use within pairing solution is investigated with emphasis on inter-user interference and using mobility scenarios, performance of the sequential algorithms are contrasted. Finally, Chapter 6 concludes the thesis.

Chapter 2

Literature Review of Assignment Problems in Full-Duplex Communications

In this chapter, we survey assignment problems in in-band full-duplex communications. For the objectives such as improving spectrum usage or decreasing latency, and under limitations of imperfect SI cancellation and inter-node interference, various assignment problems are emerged. We will review related work involving user pairing, power control, subchannel allocation and scheduling problems.

Goyal et al. propose a scheduling algorithm that uses half-duplex as default mode of operation and switches to full-duplex operation only when performance gain is anticipated [11]. They provide formulations to determine conditions for uplink and downlink full duplex gain for the cellular scenario. Then they calculate a utility index which they use to formulate an optimization problem to choose operation mode.

In [16], resource allocation problem is formulated using game theory. In the context of full-duplex resources of transmit power level, subchannel and user

pairing, a payoff function is defined using uplink and downlink channel capacities. For base station topology, there is a trade-off between transmit power and rates. Transmit power is proportional with capacity in the same direction but degrades capacity of the other direction by increasing either SI or inter-node interference. Authors specify the condition for existence of a Nash equilibrium in terms of SI cancellation for this noncooperative game. An iterative algorithm is proposed that uses water filling algorithm at each step to adjust power levels and an argmax condition to update optimum pair allocations.

A heuristic algorithm for assignment problem on distance metric is proposed by Bae et al in [17]. The study covers bidirectional and three-node full-duplex topology for IEEE 802.11ax and incorporates a multi-cell scenario. Authors first characterize the system and determine rate regions with respect to mobile station distances. Then they elect threshold distance values for the two operation modes and SI mitigation levels. They define space scheduling algorithm that compares node distances to threshold values and assign FD or HD operation accordingly. Authors point out that three-node topology performs better than bidirectional FD when SI cancellation is less than 100 dB. They report 1.8 times increase over HD in downlink but also state that uplink gains are not achieved. By comparing the results with previous works reviewed previously, it can be concluded that this low complexity approach is not as effective for sum rate maximization problem. Additionally how node distances are acquired is not presented.

Another low complexity solution is formulated by Di et al. which presents a resource allocation method to optimally allocate subcarriers to uplink downlink pairs for a single cell full-duplex network [18]. The solution uses matching theory with three sides and solves power allocations separately.

The assignment problem can be solved in a less flexible form and engineered to be used in specific location. In [19] using geographical information, authors determine isolated regions that have high signal attenuation with respect to each other. First they extract spatial characteristics of a given well defined area using radio maps. For example, buildings are regarded as obstructions for outdoor scenarios and walls can segregate rooms for indoor scenarios. The regions that

they form are dependent on base station deployment positions. Then authors systematically calculate a parameter called mitigation factor which is used to relate inter node interference between regions and solve resource allocation problem using pre-calculated data for given geographical locations. Authors assume using localization services provided by infrastructure. We note that localization services provided such as OTDOA, E-CID offer various levels of accuracy which can influence proposed heuristic assignment procedure provided, and some services such as GNSS are not universally implemented in user equipment.

Approaches for assignment problems widely assume that required set of parameters are available. However this presumption is questionable due to its practicality. The concern is expressed by Nam et al. for the case which full channel state information is not inaccessible for scheduling [20]. The study first revisits the resource allocation problem with full CSI and formulates a sequential algorithm. Downlink allocations use linear assignment problem and water filling for node and power selection respectively. For uplink allocations a dual optimization method is used. The combined algorithm first executes one of the two, fixes the subchannel allocation and solves the other direction.

Limited CSI discussion acknowledges the difficulties and associated overhead of measurement and feedback procedures. Opportunistic feedback principle is used to constraint overhead. A frame structure is proposed that defines a training sequence, followed by time slots for feedback and scheduling. Time slots designated for feedback represent predetermined threshold values. Mobile stations select appropriate time slots according to their measurements from training sequence and transmit their identifier. The signals during this period are also used by downlink nodes to identify corresponding inter-node interference to said node. Base station then announces uplink scheduling with power levels. During the second round, downlink nodes send their desired resources similar to uplink case with different threshold values. Downlink scheduling concludes the resource process. Proposed scheme allows multiple mobile stations to access the channel at the same time, resulting in collisions. To alleviate such cases authors try to calculate threshold values to minimize collision probabilities. Results indicate that increasing number of slots thus enlarging set of thresholds increase the performance, however

overhead also increases decreasing the efficiency.

2.1 Contributions of the Thesis

In this thesis, we consider user pairing problem in a single cell topology with full-duplex base station and legacy half-duplex mobile stations. Performance evaluations of pairing algorithms are provided. A closed form solution is formulated for user capacity distribution under random pairing which is used to calculate the sum rate distribution.

We investigate a practical issue of obtaining channel state information, specifically inter-user interference values. A learning procedure which reduces the overhead by more than 80% is presented for this often overlooked problem. Then using this learning procedure we tackle an unexposed problem: user mobility in full-duplex networks. Unlike stationary environments, the pairing problem needs to constantly update the channel state information received from mobile nodes. Complexity of model based solutions to user selection problem for learning process is discussed, and a heuristic algorithm with nonuniform weighted random learning is proposed. The algorithm is a stochastic approach to the learning process and uses receiver reports to estimate other nodes to provide more than 60% faster convergence to the optimum solution compared to baseline algorithms.

Chapter 3

Problem Formulation

In this chapter, we first introduce the operation mode for full duplex wireless network with half duplex nodes. Then we define the relevant communication parameters and performance metrics for the user pairing problem. We present solutions to the pairing problem and lastly, evaluate their performances.

3.1 Full Duplex Operation

We consider full-duplex capable base station (BS) and half-duplex user equipment (UE) in a single cell wireless network. Base station has the ability to suppress self-interference sufficiently to ensure reliable communication. Each and every user equipment utilizes a traditional half-duplex transceiver.

The operation between BS and UE are based on an enhanced version of time-division duplexing (TDD) mode. In TDD spectrum resources are partitioned into time slots of fixed duration. A number of time slots are grouped together to form a frame. The structure of the frame defines assignment of slots for uplink and downlink transmission, as well as slots reserved for special purposes. In traditional synchronous TDD, uplink and downlink transmissions occur in mutually exclusive time slots, and BS and UE switch between transmit and receive modes according

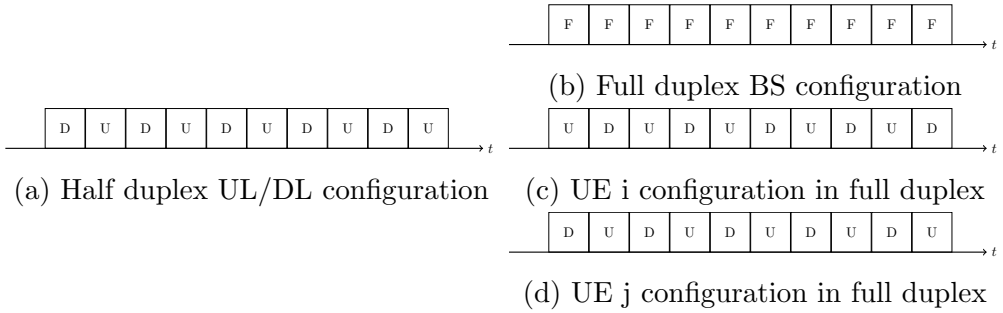

(b) Full duplex BS configuration

(a) Half duplex UL/DL configuration

(c) UE i configuration in full duplex

(d) UE j configuration in full duplex

Figure 3.1: Half-Duplex and Full-Duplex TDD Mode Configuration

to frame structure. In this scenario we assume a modified TDD operation where HD UE performs duplexing, while FD capable BS jointly transmits and receives. An example frame configuration is given in Figure 3.1 for half duplex and full duplex TDD. Time slots for DL and UL are abbreviated as D and U respectively. In figures 3.1b, 3.1c, 3.1d BS is set up for full duplex operation at the same frequency with two HD users UE i and UE j.

The ability of assigning two users to the same resource block premises increasing utilization and doubling spectral efficiency. However such systems also bring performance constraints as we will investigate in the following section.

3.2 Scenario

An illustration of the single cell scenario with half-duplex UE operation is depicted in Figure 3.2.

Here uplink node UE i and BS are transmitting simultaneously with transmit powers P_i and P_{BS} respectively. Channel gain from UE i to BS is $g_{i,BS}$, from BS to UE j is $g_{BS,j}$, and from UE i to UE j is $g_{i,j}$. The scenario also incorporates two sources of interference.

The first source is due to self-interference. In order to counteract this interference component, base station utilizes cancellation methods described in previous chapter. In this work self-interference cancellation is assumed to be imperfect

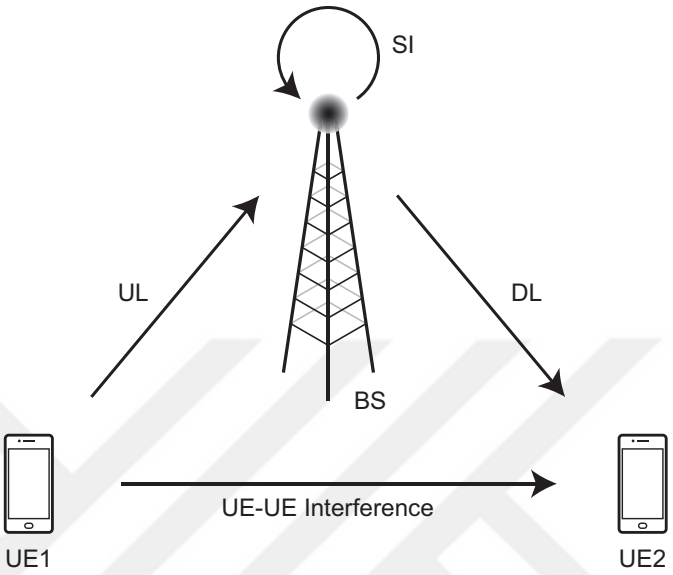

Figure 3.2: Scenario

at the full-duplex capable BS. Self-interference suppression stages are aggregated into a parameter self-interference cancellation coefficient (SI_C). The remaining portion is residual self-interference SI_R which is injected to receiver chain of BS as interference. SI cancellation process is modeled as:

$$\mathrm{SI}_R = \mathrm{SI} - \mathrm{SI}_C \tag{3.1}$$

The second source is inter-node interference which is a consequence of the scheme with half-duplex UE. From UE j perspective, transmission of UE i is added on top of signal from BS.

In order to assess we use signal to interference plus noise ratio (SINR).

Uplink SINR:

$$\gamma_{\mathrm{UL}} = \frac{P_i \; g_{i,BS}}{N_{BS} + \mathrm{SI}_R} \tag{3.2}$$

Downlink SINR:

$$\gamma_{\mathrm{DL}} = \frac{P_{BS} \; g_{BS,j}}{N_j + P_i \; g_{ij}} \tag{3.3}$$

Shannon's channel capacity per unit bandwidth is given by

$$C = \log_2 (1 + \text{SINR}) \quad \text{in b/s/Hz} \tag{3.4}$$

Corresponding UL and DL capacities are:

$$C_{\text{UL}} = \log_2 \left(1 + \frac{P_i \ g_{i,BS}}{N_{BS} + \text{SI}_R} \right) \tag{3.5}$$

$$C_{\text{DL}} = \log_2 \left(1 + \frac{P_{BS} \ g_{BS,j}}{N_j + P_i \ g_{ij}} \right) \tag{3.6}$$

As we can infer from figures residual self interference is a limiting factor on UL performance while DL rates are restricted by inter-UE interference arising from channel gain between nodes i and j. As a consequence UL performance relies on SI suppression technology, however DL performance is directly related to interference path $g_{i,j}$. As the choice of UE pairs for UL and DL determine the set of channel gain values by means of scheduling, the association for such pairs is a decision parameter. In the next section we discuss how it can be exploited to regulate network performance.

3.3 User Pairing

A reduced example scenario with four nodes for user pairing problem is illustrated in Figure 3.3. First pairing allocation (Figure 3.3a) combines pairs as (UE1,UE2) and (UE4,UE3) as downlink and uplink pairs respectively, whereas second allocation (Figure 3.3b) favors (UE1,UE3) and (UE4,UE2). Inter-node interference path of pairs are shown with dashed lines and for given topology. Due to link geometry, pairing (a) exhibits shorter distance between associated UE, thus larger interference from UL nodes to DL nodes. As a result it can be inferred that pairing (b) is more efficient than (a) as it can provide better downlink SINR.

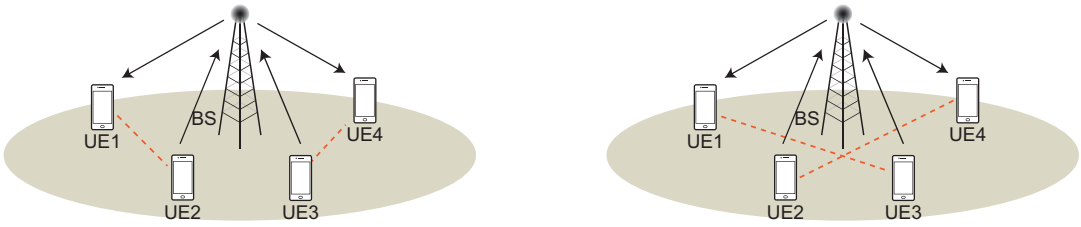

(a) (b)

Figure 3.3: An example topology with two pairing configurations

The objective is to obtain an pairing in which the cumulative network capacity is maximized. We assume that all channel gain parameters are available at the scheduler so channel capacity for each possible pair can be calculated. The cell consists of N number of UEs, so an N by N matrix with entries c_{ij} is formed. Applying utility based scheduling with utility function selected as $U(i,j) = c_{i,j}$, sum of rates are maximized. We assume each node has the same priority and has full transmit buffer.

UE assignment problem can be formulated as a bipartite graph matching with the following model. User pairs are represented with a binary variable x_{ij} which corresponds to a pairing of transmitter i and receiver j if $x_{ij} = 1$. X is the pairing matrix where rows and columns correspond to transmitting and receiving users respectively. Therefore the problem can be constrained to take integer values between 0 and 1 inclusive (3.10). In addition, each user should have an opportunity to receive and transmit so there should be at least one nonzero value at each row and column. Furthermore, only one user can transmit to a given user so each row and column can have at most one nonzero value. Last two constraints, (3.8) and (3.9) state that summation of each row and column should be precisely 1.

$$\text{Maximize} \quad \sum_{i=1}^{N}\sum_{j=1}^{N} c_{ij}\ x_{ij} \tag{3.7}$$

$$\text{Subject to} \quad \sum_{i=1}^{N} x_{ij} = 1,\ j = 1, \ldots, N \tag{3.8}$$

$$\sum_{j=1}^{N} x_{ij} = 1,\ i = 1, \ldots, N \tag{3.9}$$

$$x_{ij} \in \{0, 1\},\ i, j = 1, \ldots, N \tag{3.10}$$

3.4 Solution Methods

User pairing problem described in the previous section can be solved using following assignment methods.

3.4.1 Linear Assignment

This problem structure is linear assignment problem and can be solved with Hungarian algorithm.

As number of users increase, the size of utility matrix thus execution time grows. We use another linear assignment problem algorithm called Shortest Augmenting Path Algorithm (LAPJV) by Jonker and Volgenant [21]. Although LAPJV algorithm has the same worst case complexity as Hungarian algorithm, due to its initial preprocessing phase, on the average it is slightly faster than its counterpart for large problems with dense matrices [22].

3.4.2 Random Assignment

Random assignment is regarded as unmanaged scheduling configuration and used as baseline for evaluating effectiveness of a user selection algorithm. As this method does not contain any scheduling preference, it is regarded as the worst case selection for this scenario.

This method is similar to concatenating half duplex UL and DL user scheduling configurations, given a set of nodes corresponding to time slots in one direction, a random permutation of the same set is assigned to nodes for the other direction. Additionally assignment of the same node to both UL and DL is prohibited i.e $x_{i,i} = 0,\ \forall i = \{1, \ldots, N\}$.

3.4.3 Gale-Shapley Algorithm

A matching theory approach is used to simplify the user selection problem by transforming sum rate maximization problem into a stable matching problem. The utility matrix is transformed into ordered preference lists for each node. Preference lists include every possible matching ranked by their estimated rate in descending order. In other words from user perspective, pairing with the node in first entry of this list would achieve the best rate. The objective is to find a stable matching, and we use Gale-Shapley algorithm [23] to solve this problem. Algorithmic complexity is $O\left(n^2\right)$ for when the cardinality of both sides are equal [24].

As explained previously, the downlink performance heavily relies on the scheduling, furthermore expected uplink traffic demand and targeted uplink spectral efficiency is lower than their downlink counterparts. Therefore downlink preferences are prioritized with the expectation of a larger sum rate.

Achieving global maximum of sum rate is unlikely with this algorithm as the objective function does not consider system utility. On the other hand computational complexity is lower than of max sum rate algorithm, also the overhead

associated with channel estimations to interferers can be compressed with this method.

3.4.4 Fairness

As the user association problem is structured to improve the aggregate utility of the cell, scheduling decisions involving nodes are processed as a whole and does not necessarily represent performance of individual nodes. Therefore objective function can inhibit a node by pairing it with a less favorable complement to improve throughput of another node if the resulting utility is increased. Such an arrangement favors efficiency and reduce fairness among users.

In our scenario, network topology, in particular link geometry and distribution of UE, can be a limiting factor for performance of particular nodes [11]. As a consequence, scheduler is constrained in providing a fair allocation to the nodes. For instance, a node that encounters heavy inter node interference regardless of the pairing configuration will have a limited range of achievable rates. Considering such instances it can be inferred that an egalitarian approach such as max-min fairness can disrupt efficiency and limit full duplex capacity gain.

In this work, to examine fairness for user association problem we replace the objective function (3.7) with a logarithmic utility function $U(i,j) = \log(c_{ij})$ to obtain a proportionally fair resource distribution [25].

$$\sum_{i=1}^{N}\sum_{j=1}^{N} \log(c_{ij})\ x_{ij} \tag{3.11}$$

3.5 Simulation Results

In this chapter, we evaluate performance of pairing methods with a small cell scenario. Simulation parameters are configured based on the scenario 2 of 3GPP

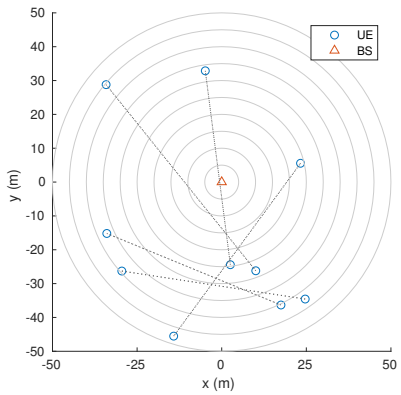

Figure 3.4: Visualization of UE pairings for an example topology

specification [26] are given in Table 3.1. We assume full buffers with heavy traffic in a single cell environment.

Table 3.1: Simulation Parameters

Parameter	Value
Cell radius	50 m
UE Placement	Uniformly random
Maximum Pico TX power	24 dBm
Maximum UE TX power	23 dBm
Thermal noise density	-174 dBm/Hz
BS-UE Path loss model	$\mathrm{PL}_{\mathrm{LOS}}(R) = 103.8 + 20.9 \log_{10}(R)$ $\mathrm{PL}_{\mathrm{NLOS}}(R) = 145.4 + 37.5 \log_{10}(R)$
LOS probability	$0.5 - \min(0.5, 5\exp(-0.156/R))$ $+ \min(0.5, 5\exp(-R/0.03))$
UE-UE Path loss model	$R \leq 50m$;PL $= 98.45 + 20 \log_{10}(R)$ $R > 50m$;PL $= 175.78 + 40 \log_{10}(R)$
Noise figure	9 dB (UE) 13 dB (BS)
Shadowing std deviation BS and UE	3dB (LOS) 4dB (NLOS)

Abbreviations for pairing schemes used figures are given in Table 3.2.

Table 3.2: Abbreviations used in figures

MR	Max sum rate
RN	Random pairing
HD	Half-duplex
PF	Proportionally fair
GS	Stable matching

The following figures show cumulative distribution of average sum capacities within a cell for 100 dB SI cancellation.

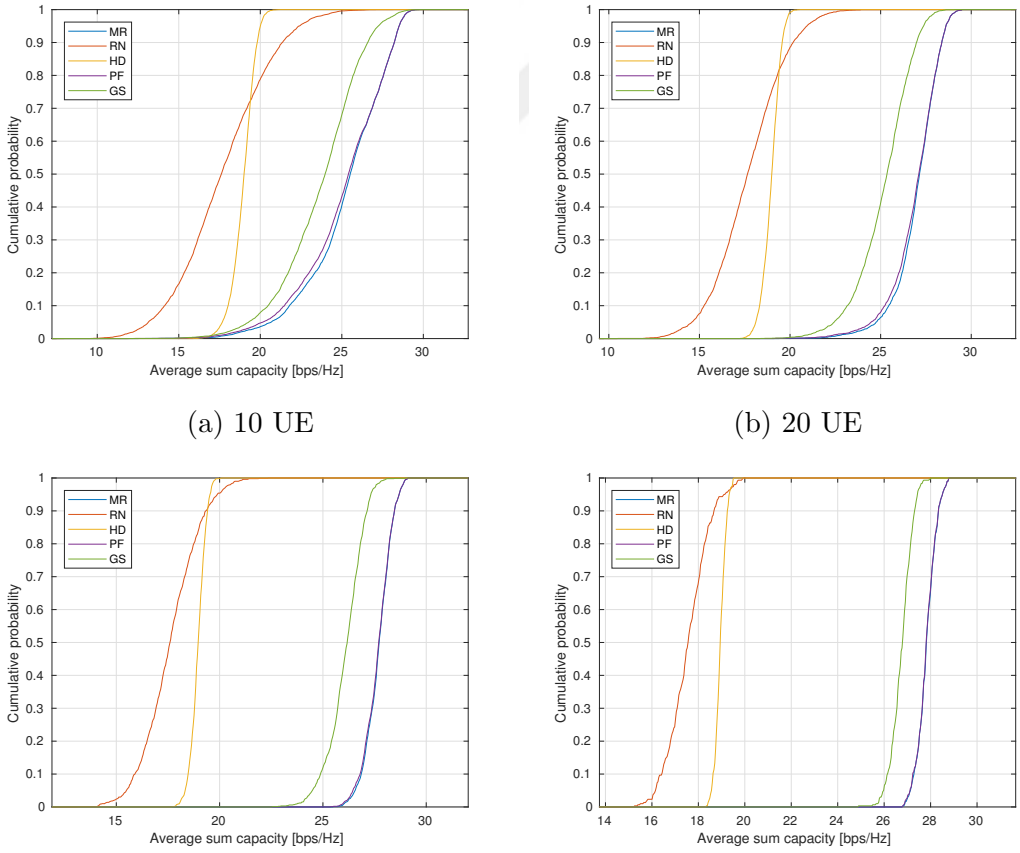

(a) 10 UE

(b) 20 UE

(c) 40 UE

(d) 100 UE

Figure 3.5: Cumulative distribution of average sum capacity for 100 dB SI suppression

In Figure 3.5, it can be seen that sum rates that full-duplex pairings achieve have larger variance than half-duplex case. Performance of random pairing gradually gets worse as number of mobile stations increases. As we have noted in fairness section, the topology influences rate distribution greatly such that obtaining a more fair allocation decreases sum rate utility. We observe that proportionally fair pairing follows max sum rate algorithm closely.

Figure 3.6 illustrates distribution of pair distances for 20 UE and 110 dB SI suppression of 50000 pairs (10^5 nodes).

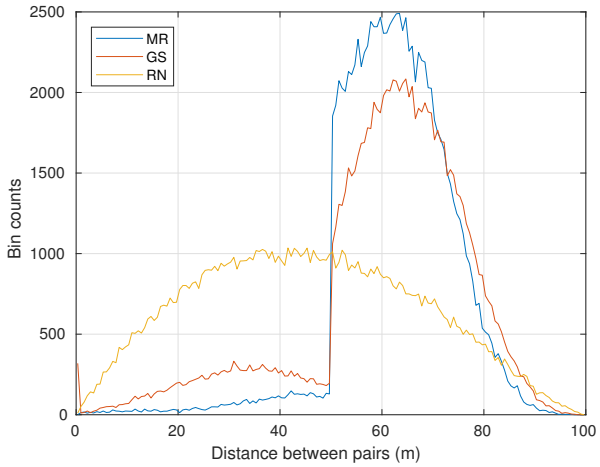

Figure 3.6: Pair distances

We observe that random pairing behaves arbitrarily and follows node placement distribution. Max sum rate algorithm has the least amount of pairs that are closer than 50 m. Stable matching results in largest amount of pairs with separation over 80 m however the overall sum rate performance is inferior than previous algorithm which can be verified from Figure 3.5b.

In the following simulations we compare average sum rate achieved using full-duplex with half-duplex to calculate gain percentage for numerous user density cases.

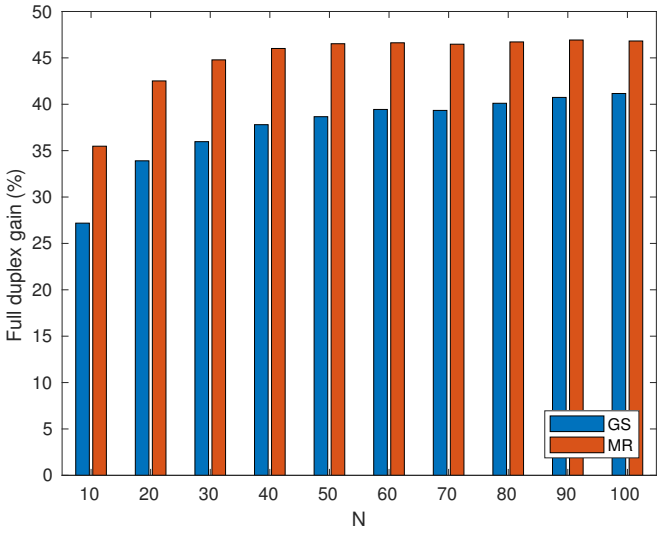

Figure 3.7: Sum rate improvement over half-duplex for 100 dB SI suppression

For 100dB SI cancellation, max rate algorithm and stable matching reach 46.82 % and 41.16 % improvement respectively as number of mobile stations increase to 100. Random pairing for this environment results in approximately 10 % sum rate loss.

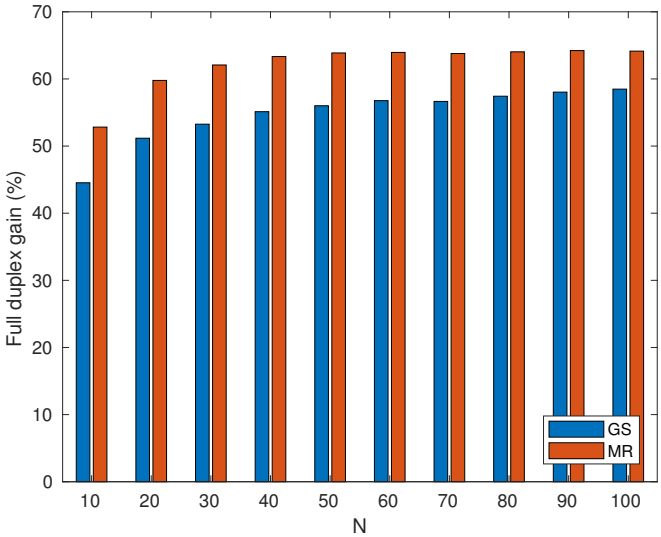

Figure 3.8: Sum rate improvement over half-duplex for 110 dB SI suppression

For 110dB SI cancellation, max rate algorithm and stable matching reach 64.14 % and 58.48 % improvement respectively as number of mobile stations increase to 100. Random pairing for this environment results in approximately 10 % sum rate gain which is consistent with the improvement max rate algorithm the change 100 dB.

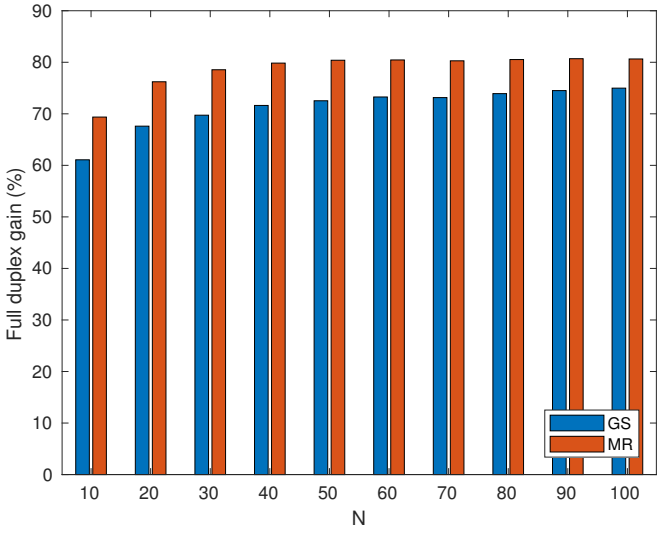

Figure 3.9: Sum rate improvement over half-duplex for 120 dB SI suppression

For 120dB SI cancellation, max rate algorithm and stable matching achieve 80.64 % and 74.98 % improvement respectively. The performance difference between two algorithms decrease as SI cancellation improves diminishing difference between uplink and downlink rates. Random pairing attains approximately 26 % sum rate gain over half-duplex.

In Figure 3.10 5th percentile of sum rate improvement with respect to number of users is given for 100 dB SI cancellation.

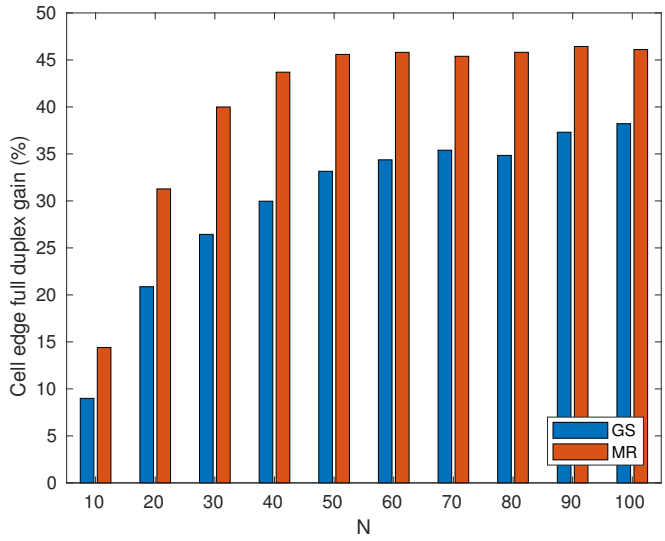

Figure 3.10: Cell edge sum rate improvement over half-duplex for 100 dB SI suppression

In contrast to results in Figure 3.7, it is observed that full-duplex gains are not equally distributed for 10, 20, 30 users. Additionally, performance difference between stable matching and max sum rate algorithms is apparent.

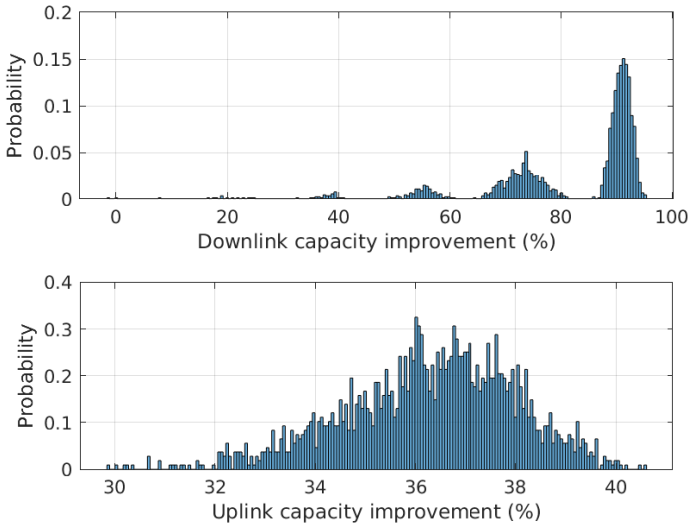

Figure 3.11: Histogram of capacity improvements per node for 20 UE and 110 dB SI suppression

In Figure 3.11, we decompose the sum rate gains to its uplink-downlink components and plot histogram of capacity improvement per node for max sum rate algorithm. We observe that uplink performance is influenced by SI and node distribution as expected. However the downlink performance is not homogeneous and cluster formations at certain rates are present. We will be further investigating underlying reasons in the next chapter using an analytic approach.

Chapter 4

Throughput Analysis Under Random Pairing

Results of user pairing problem indicate that random pairing scheme exhibits low performance. In this chapter to investigate theoretical basis of full duplex scenario, we derive an analytic model through distance, path loss distributions, formulation SINR and calculation of capacity.

4.1 User Distribution

We consider a circular cell of radius B with a BS at the center (0,0). Users are distributed with uniform density. The PDF of position of a UE in Cartesian coordinates are:

$$f_{XY}(x,y) = \begin{cases} \frac{1}{\pi B^2} & x^2 + y^2 \leq B^2 \\ 0 & otherwise \end{cases} \tag{4.1}$$

In order to derive distance dependent path loss functions we need two variables:

- Distance between BS and UE (R)
- Distance between UE and UE (D)

R is the random variable for distance between BS and UE and has the following PDF:

$$f_R(r) = \begin{cases} \frac{2}{B^2} r & 0 \leq r \leq B \\ 0 & otherwise \end{cases} \tag{4.2}$$

Random variable for angle between BS and UE Θ is uniform in interval $[0, 2\pi)$.

The distance distribution for two points is derived for uniform distribution in $\mathbb{R}^2$ space by following the derivation by Moltchanov for two random points in a region [27].

Crofton's formula for two points [28]. P_1 denotes the probability that one point is chosen at random in the boundary of the cell. P is the probability that distance between two points is between l and $l + \Delta l$. A is the area of the cell.

$$dP = 2\left(P_1 - P\right)\frac{dA}{A} \tag{4.3}$$

$$P_1 = \frac{(2ldl)\cos^{-1}\left(l/2B\right)}{\pi B^2} \tag{4.4}$$

Here ldl is the line segment that corresponds to the probability P, $2\cos^{-1}\left(l/2R\right)$ is the angle that this line segment can be rotated and πR^2 in the denominator normalizes the probability with respect to cell area. If P_1, and A is placed into formula

$$B\,dP + 4P\,dB = \frac{8l\Delta l\cos^{-1}\left(l/2B\right)}{\pi B^2} \tag{4.5}$$

The result is obtained by integration of this expression. Using variable d we can express corresponding PDF in $0 \leq d \leq 2B$ as;

$$f_D(d) = \frac{2d}{B^2}\left[\frac{d}{\pi B}\sqrt{1-\frac{d^2}{4B^2}} - \frac{2}{\pi}\cos^{-1}\left(\frac{d}{2B}\right)\right] \tag{4.6}$$

For a boundary $B = 50\,\mathrm{m}$ the PDF is calculated as follows

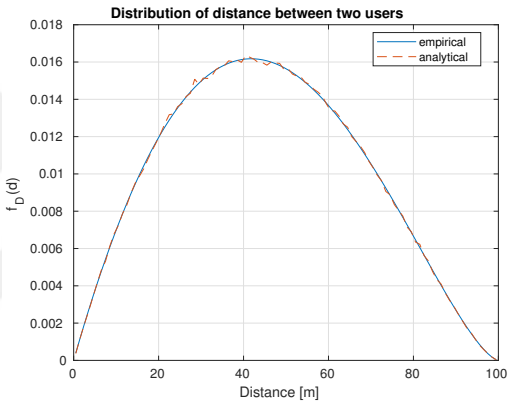

Figure 4.1: Distribution of distance between two points in a cell

The conditional distance distribution given BS-UE separation $f_{D|R}(d|R = r)$ is calculated as follows:

For uniformly distributed nodes, two cases form a partition of sample space. An illustration where a node is separated from BS by r_1 $(R = r_1)$ can be seen in the Figure 4.2.

Due to symmetry of the topology, angular orientation can be left out and the first node is fixed at -x direction. The two cases are separated by the radius the circle which is centered on first UE and its edge intersects with the cell boundary at only one point. In Figure $d = l_1$ and $d = l_2$ are inside and outside of that circle respectively.

The distance distribution inside this circle is a scaled version of $f_R(r)$ with radius $\mathrm{B} - r_1$ and the center is shifted to position of first node.

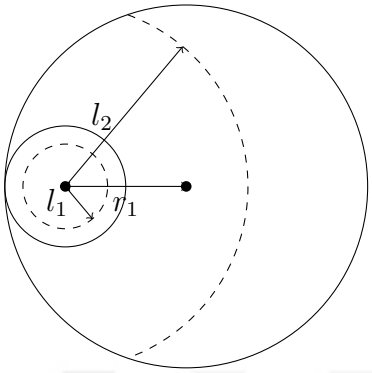

Figure 4.2: Illustration of distance distribution given r_1

For the second case, the probability of distance d corresponds to an arc. End points of this arc are determined with trigonometry. Lastly factoring two cases with their probabilities leads to:

$$f_{D|R}\left(d|R=r_1\right)\begin{cases}\frac{2d}{B^2} & 0\leq d\leq B-r_1\\ \frac{2d}{\pi B^2}\cos^{-1}\left(\frac{d^2+{r_1}^2-B^2}{2r_1 d}\right) & B-r_1<d\leq B+r_1\end{cases} \tag{4.7}$$

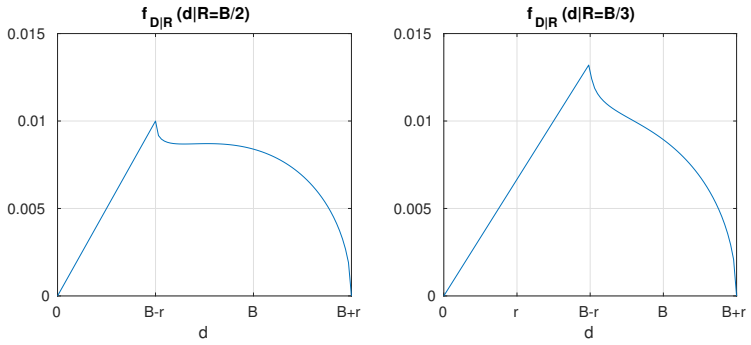

Figure 4.3: Conditional distribution examples

4.2 Distribution of Path Loss

The distribution of the path loss is calculated for the model in the form $PL = A_1 + A_2 \log_{10}(r)$ where A_1 and A_2 are constants and r is the distance between

source and destination in kilometers. We first represent this model in meters and natural logarithm.

$$\begin{aligned} PL &= (A_1 - 3A_2) + A_2 \log_{10}(d) \\ &= (A_1 - 3A_2) + \frac{A_2}{\log(10)} \log(d) \end{aligned} \tag{4.8}$$

For brevity two constants $K_1 = A_1 + 3A_2$ and $K_2 = A_2/\log(10)$ are defined and d is nonnegative by definition. By inverse transform method the CDF and PDF of the loss function are as follows:

$$F_Y(y) = F_X\left(\exp\left(\frac{y - K_1}{K_2}\right)\right) \tag{4.9}$$

$$f_L(l) = \frac{1}{K_2} \exp\left(\frac{l - K_1}{K_2}\right) f_D\left(\exp\left(\frac{l - K_1}{K_2}\right)\right) \tag{4.10}$$

$f_L(l)$ is defined for $l \leq A_1 + A_2 \log_{10}(2r/10^3)$, which corresponds to domain $0 \leq d \leq 2B$. A lower bound on loss can be set as the probability of small separations ($d < 1m$) is negligible. This bound can also be justified with the minimum distance requirements in the network topology models.

4.2.1 BS-UE Path Loss

The path from BS to UE or UE to BS is distributed with the random variable R and the distribution of path loss can be easily derived by replacing $f_D(d)$ with $f_R(r)$ for $l \leq K_1 + K_2 \log(R)$

$$\begin{aligned} f_L(l) &= \frac{1}{K_2} \exp\left(\frac{l - K_1}{K_2}\right) f_R\left(\exp\left(\frac{l - K_1}{K_2}\right)\right) \\ &= \frac{2}{B^2 K_2} \exp\left(2\frac{l - K_1}{K_2}\right) \end{aligned} \tag{4.11}$$

Using the model $PL = 103.8 + 20.9 \log_{10}(R)$ the received signal level at the UE $f_S(s) = P_{BS} - PL$ is as follows.

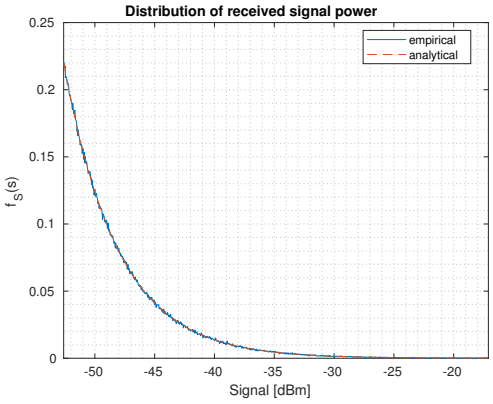

Figure 4.4: BS-UE path loss

Root mean square error between simulation and analytical formulation is 9.3566e-04 (10^6 sample points, 10^3 histogram bins).

4.2.2 UE-UE Path Loss

The interference component for the downlink transmission is derived with distance distribution. For brevity let l^*

$$l^* := -\frac{K_1 - l}{K_2}$$

Replacing $f_D(d)$ with the expression in previous section :

$$f_L(l) = -\frac{1}{K_2} \exp(l^*) \left[\frac{4}{\pi B^2} \exp(l^*) \sin^{-1}\left(\frac{1}{2B} \exp(l^*) \right) - \frac{2}{B^2} \exp(l^*) \right] - \frac{1}{K_2} \exp(l^*) \left[\frac{1}{\pi B^4} \exp(2l^*) \sqrt{4B^2 - \exp(2l^*)} \right] \quad (4.12)$$

Illustration of this distribution with the PL model $PL = 148.03 + 40 \log_{10}(d)$:

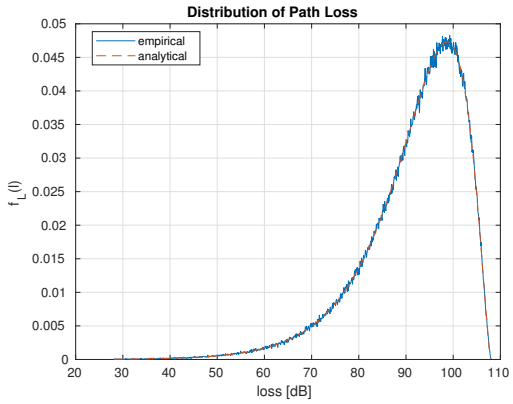

Figure 4.5: Distribution of path loss with respect to distance

The path loss model of interest has two cases

$$PL = \begin{cases} 98.45 + 20\log_{10}(d/1e3) & d \leq 50 \\ 55.78 + 40\log_{10}(d) & d > 50 \end{cases} \tag{4.13}$$

A combination of the two partitions is expressed with a sum of product of $f_L(l)$ times an indicator function which is valid in given domains $[0, 50)$ and $[50, 2B]$. Interference level at the receiver UE $f_I(i) = P_{UE} - PL$ is as follows.

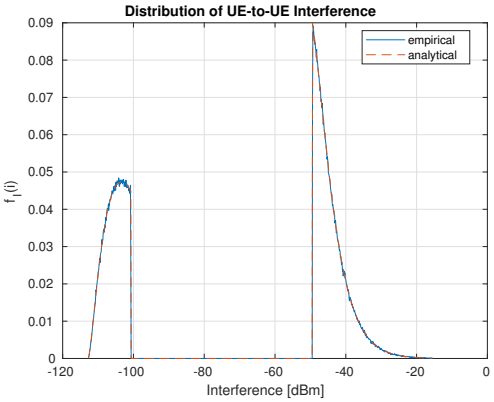

Figure 4.6: UE-UE interference distribution

Root mean square error between simulation and analytical formulation is

8.7954e-04 (10^6 sample points, 10^3 histogram bins).

4.3 Distribution of SINR

4.3.1 Uplink SINR

Uplink SINR is given as

$$\gamma_{\mathrm{UL}} = \frac{P_i \; g_{i,BS}}{N_{BS} + \mathrm{SI_R}} \tag{4.14}$$

Transmit power level of UE, noise level and residual self interference can be assumed constant. Channel gain is also simplified by removing antenna gain and shadow fading effect. Then the random variable S can be derived from the random variable -R by shifting its PDF.

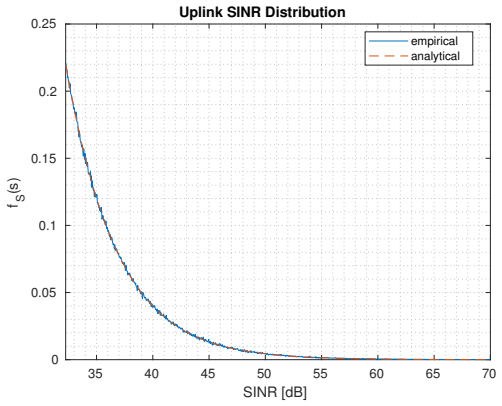

Figure 4.7: Uplink SINR distribution

4.3.2 Downlink SINR

Downlink SINR is given as

$$\gamma_{\mathrm{DL}} = \frac{P_{BS} \; g_{BS,j}}{P_i \; g_{i,j} + N_j} \tag{4.15}$$

In dB units, it can be restated, noting the power sum of noise and inter-node interference terms.

$$\Gamma = (P_{BS} - K_{1a} - K_{2a}\log(R)) - 10\log_{10}\left(N + 10^{(P_{UE} - K_{1b} + K_{2b}\log(D))/10}\right) \quad (4.16)$$

Noise can be ignored under the condition that it is negligible compared to interference power.

$$N \ll 10^{\frac{P_{UE} - K_{1b} + K_{2b}\log(D)}{10}} \quad (4.17)$$

In addition to simplifications described in Uplink SINR calculation, noise power is assumed to be negligible compared to interference component, and the expression is evaluated in dB scale:

$$\begin{aligned}\Gamma &= (P_{BS} - g_{BS,j}) - (P_i - g_{i,j}) \\ &= (P_{BS} - K_{1a} - K_{2a}\log(R)) - (P_i - K_{1b} - K_{2b}\log(D)) \\ &= (P_{BS} - K_{1a} - P_i + K_{1b}) + (K_{2b}\log(D) - K_{2a}\log(R))\end{aligned} \quad (4.18)$$

Note that random variables R and D are not independent thus difference of two channel gain random variables are evaluated using their joint probability. Loss constants K_1 and K_2 follows the definition in section 4.2 while subscript a and b are used for nominator and denominator of signal to interference ratio respectively. Let K be a constant and $K = K_{2a}/K_{2b}$ then define a random variable Z.

$$Z = \log(D) - K\log(R) = W - U \quad (4.19)$$

$$\begin{aligned}f_U(x) &= \frac{1}{K} e^{\frac{x}{K}} f_R\left(e^{\frac{x}{K}}\right) && -\infty \le x \le K\log(B) \\ &= \frac{2\exp\left(\frac{2x}{K}\right)}{KB^2} && -\infty \le x \le K\log(B)\end{aligned} \quad (4.20)$$

$$f_{W|U}\left(y|U=x\right)=\begin{cases}\frac{2e^{2y}}{B^2} & -\infty\leq y\leq\log\left(B-e^{\frac{x}{K}}\right)\\ \frac{2e^{2y}}{\pi B^2}\cos^{-1}\left(\frac{e^{2y}+e^{\frac{2x}{K}}-B^2}{2e^{\frac{x}{K}}e^{y}}\right) & \log\left(B-e^{\frac{x}{K}}\right)<y\leq\log\left(B+e^{\frac{x}{K}}\right)\end{cases} \tag{4.21}$$

From conditional probability $f_{W|U}\left(w|U=u\right)$, we calculate joint probability density function.

$$f_{W,U}\left(w,u\right)=f_{W}\left(w|U=u\right)f_{U}\left(u\right) \tag{4.22}$$

$$f_{W,U}\left(w,u\right)=\begin{cases}\frac{4}{KB^4}e^{2w}e^{\frac{2u}{K}} & -\infty\leq w\leq\log\left(B-e^{\frac{u}{K}}\right)\\ \frac{4e^{2w}e^{\frac{2u}{K}}}{\pi KB^4}\cos^{-1}\left(\frac{e^{2w}+e^{\frac{2u}{K}}-B^2}{2e^{\frac{u}{K}}e^{w}}\right) & \log\left(B-e^{\frac{u}{K}}\right)<w\leq\log\left(B+e^{\frac{u}{K}}\right)\end{cases} \tag{4.23}$$

Using joint probability distribution function, we can evaluate difference of two correlated random variables using (4.24).

$$f_{Z}\left(z\right)=\int f_{W,U}\left(\tau,\tau-z\right)d\tau \tag{4.24}$$

$f_{Z}\left(z\right)$ is a linear combination of the two cases listed below for $-\infty\leq\tau\leq K\log\left(B\right)+z$.

$$\begin{aligned}f_{Z}\left(z\right)=&\frac{4}{KB^4}e^{\frac{-2z}{K}}\int_{-\infty}^{\log\left(B-e^{\frac{\tau-z}{K}}\right)}e^{\tau\frac{2(K+1)}{K}}d\tau\\&+\frac{4}{\pi KB^4}e^{\frac{-2z}{K}}\int_{\log\left(B-e^{\frac{\tau-z}{K}}\right)}^{\log\left(B+e^{\frac{\tau-z}{K}}\right)}e^{\tau\frac{2(K+1)}{K}}\cos^{-1}\left(\frac{e^{2\tau}+e^{\frac{2(\tau-z)}{K}}-B^2}{2e^{\frac{\tau}{K}}e^{\tau}e^{\frac{-z}{K}}}\right)d\tau\end{aligned} \tag{4.25}$$

Loss function described in section 4.2.2 has two cases conditioned on the distance which sets a lower and upper bound. Integration limits should be replaced with logarithm of these bounds if they are tighter. After numerical calculation

of this PDF, SINR distribution is obtained by applying inverse transformation

$$f_\Gamma(\gamma) = f_Z\left(\left(\gamma - \left(P_{BS} - P_{UE} + K_{1b} - K_{1a}\right)\right)/K_{2b}\right)/K_{2b} \tag{4.26}$$

for the first loss model. Similarly solution for the second one follows the same procedure with subscripts c instead of b. Numerical evaluation leads to distribution in Figure 4.8.

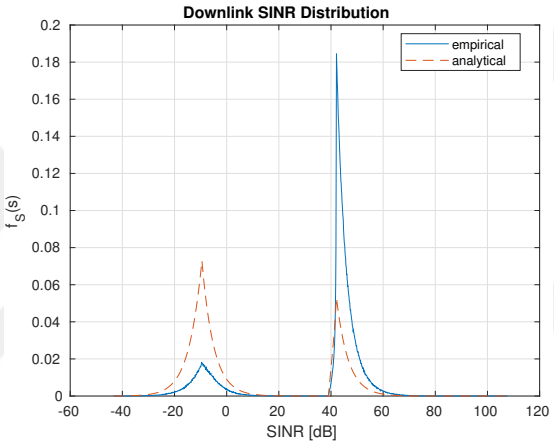

Figure 4.8: Downlink SINR distribution

4.4 Distribution of Channel Capacity

The upper bound of the bit rate per unit bandwidth for a channel is derived using calculated SINR distributions.

$$C = \log_2(1 + \text{SINR}) \tag{4.27}$$

Following transformation function relates SINR to channel capacity distibution.

$$f_C(c) = 10\log_{10}(2)\frac{2^c}{2^c - 1} f_S\left(10\log_{10}\left(2^c - 1\right)\right) \tag{4.28}$$

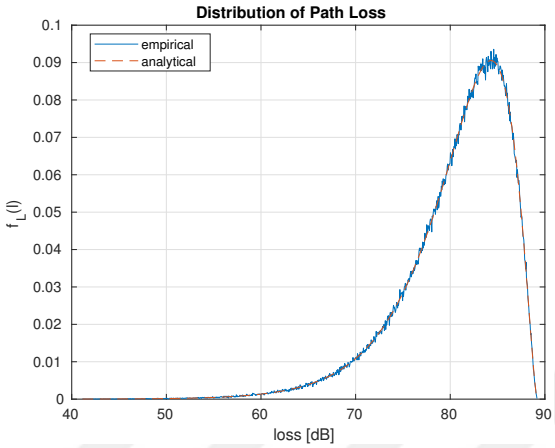

Figure 4.9: Uplink channel capacity distribution

Downlink case is numerically calculated from SINR distribution.

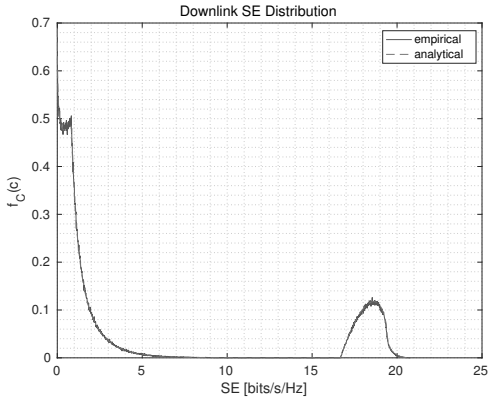

Figure 4.10: Downlink channel capacity distribution

While the downlink performance of one node can be expressed as such, in order to characterize the system performance contribution of each node should be considered. When the resources are distributed to each user evenly in time domain and mean capacity of the cell is calculated as follows where C_i^{DL} is the downlink channel capacity of user i.

$$\bar{C} = \frac{1}{N} \sum_{i=1}^{N} C_i^{\mathrm{DL}} \tag{4.29}$$

In order to derive this metric we make an assumption that capacity of each link is independent as uniform pairing method does not impose biasing. Note that if assignments in both directions are symmetrical (i.e. given $(i, j)\,;(j, i)$ is an UL&DL pair) then the random variables for their downlink capacities are dependent as their interference path distance is derived from the same random variables. On the other hand increasing number of users decrease the probability of such assignment and its influence to mean capacity.

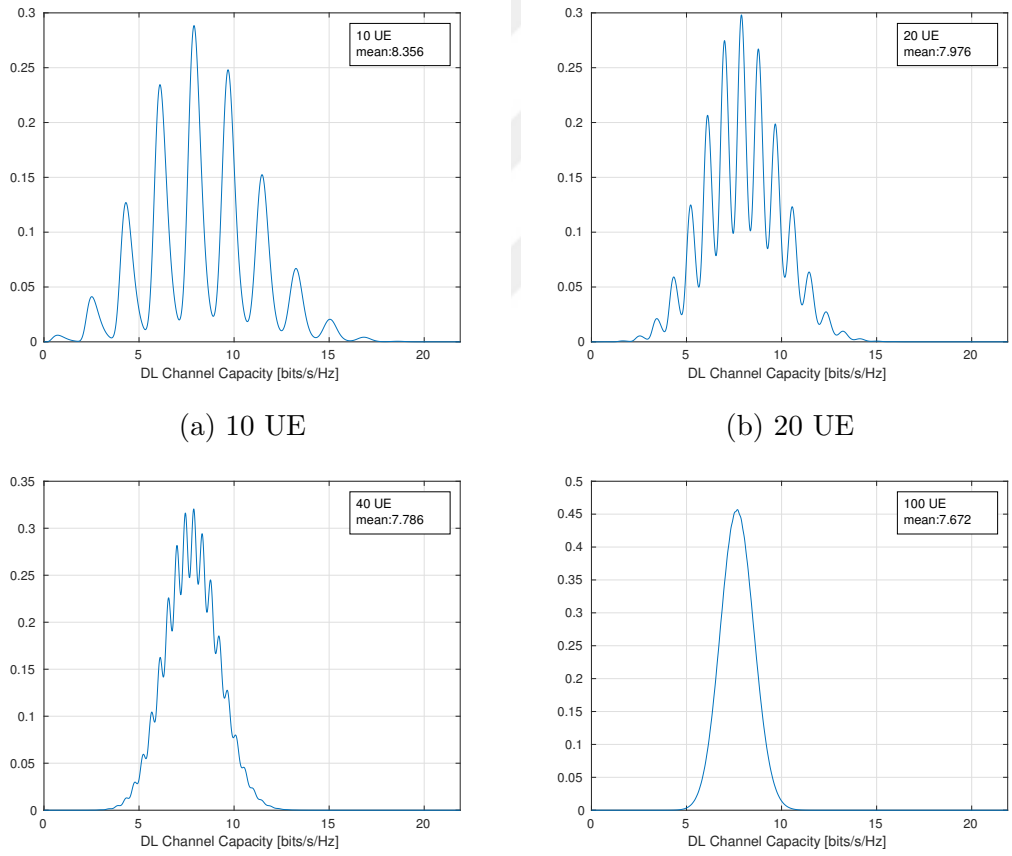

(a) 10 UE

(b) 20 UE

(c) 40 UE

(d) 100 UE

Figure 4.11: Average channel capacity with random pairing

We observe peaks at certain points which corresponds to combinatorial nature of the matching operation. The peak observed at the smallest capacity value corresponds to the case where all pairings are picked from the lower range downlink SINR distribution (i.e. smaller than 15bps/Hz). Other peaks correspond to

selecting more pairs from the high SINR region. As the number of users increase, the distribution predictably converges to the mean value with smaller variance.

In the next chapter, we will study the node pairing problem under a dynamic setting where the base station updates the node pairings based on the inter-nodal interference information received from the mobile stations. We use a learning algorithm to update the inter-nodal interference matrix.

Chapter 5

Learning-Based Pairing Algorithms under Mobility

One of the assumptions for pairing problem in previous chapters was that complete information for scheduling is always accessible. Though this presumption is common in literature, it might not be feasible for various full duplex applications.

In this chapter, we focus on a practical aspect where inter-node interference figures are not available at the scheduler and they need to be learned. Moreover in this work we consider mobility aspect of such a system where link geometries are not stationary and require constant tracking.

We first start with the concept of learning the environment, specifically inter-node interference parameters for the scenario given. We then discuss the procedure and resulting efficiency constraints. We present a generic model that represents practical aspects of the wireless network, introduce design parameters and formulate the learning problem. Lastly, we present three algorithms and assess their performance.

5.1 Learning the Environment

In Chapter 3, we have observed that performance metric is influenced by how well utility function is processed at the scheduler. Based on the observation from random pairing instance, it can be inferred that absence of channel state information is detrimental. In this section we will focus on how this information can be obtained. We first describe the structure of parameter of interest, its efficiency and requirements to establish a learning strategy.

Reference signals in 3GPP LTE are used for channel estimation and coherent demodulation at UE. Some of these are cell-specific reference signals (CRS), demodulation reference signals (DM-RS), and CSI reference signals (CSI-RS) [29]. Sounding reference signal (SRS) on the other hand is requested by BS from UE to estimate UL channel state. We assume all such methods to determine and exchange channel state information are available and utilized to characterize BS-UE links however there are some distinctions related to UE to UE interference measurement.

First let us focus on objective parameter $G = \{g_{ij}\}$; channel state information matrix for inter node interference. Given N nodes G is an $N \times N$ matrix of N^2 elements. Main diagonal of this matrix $g_{ii};\ i \in \{1, \ldots, N\}$ represent self interference. In this work we assume none of the UEs are full duplex capable, as a result self interference at UE side due to UL transmission always saturates the receiver chain, obscuring the received signal from BS. Therefore we determine main diagonal to be deterministic and for the purposes of scheduling problem assign $g_{ii} = \infty;\ i \in \{1, \ldots, N\}$ so in total we need to learn $N^2 - N$ elements.

Moreover as UL and DL transmissions share the same frequency channels, we can assume channel reciprocity, such that channel gain between node i and node j is the same in both directions. In that case we can assign $g_{ji} = g_{ij}$ and equivalently represent $G = \{g_{ij}\}$ with an upper triangular matrix which would decrease parameters of interest to $(N^2 - N)/2$.

UEs transmit reference signal which is received for every other node to estimate channel state information. Reference signal transmissions from each node occur in predefined orthogonal time slots, so that every receiver can identify the source. Furthermore during these transmissions, an in band DL operation is not permitted as the measurement would be distorted by signal from BS. Therefore channel utilization of full duplex mode cannot be achieved during these reference signal transmissions. In order to fill the matrix under channel reciprocity assumption, $N-1$ transmissions are required to be made as row vector for last node can be reconstructed from previous sequences.

In this work, we consider a centralized scheduler, in order to make an UE pairing allocation, inter node interference matrix should be present at this unit. As we have calculated previously, there are $(N^2-N)/2$ parameters to be transmitted from UEs to BS to form a utility function. Unlike reference signal transmission from UEs, feedback data transmission allows full duplex operation. Let reference signal transmissions k_{rs} bits each and feedback transmissions take k_{fb} bits per element; then every learning sequence will require $(N-1)\,k_{\mathrm{rs}}$ bits for downlink and $(N-1)\,k_{\mathrm{rs}} + ((N^2-N)/2)\,k_{\mathrm{fb}}$ bits in total for uplink channel.

The high level model for learning scheme for inter node interference at UE side for a single reference node at a given measurement event is illustrated in Figure 5.1 and can be described as follows:

1. BS elects node to transmit sounding reference signal and propagates this information to all nodes
2. UE i transmits a sounding signal at its designated slot
3. UE $j : j \in V - \{i\}$ receives the reference signal and estimates g_{ij}
4. UE j reports its estimate to BS in conformance to the feedback scheme

It is assumed that reference signal is received by any node j (i.e. no hidden nodes). Upon receiving reference signal BS that can measure the channel quality in the UL direction as in current system implementation. After scheduling decisions

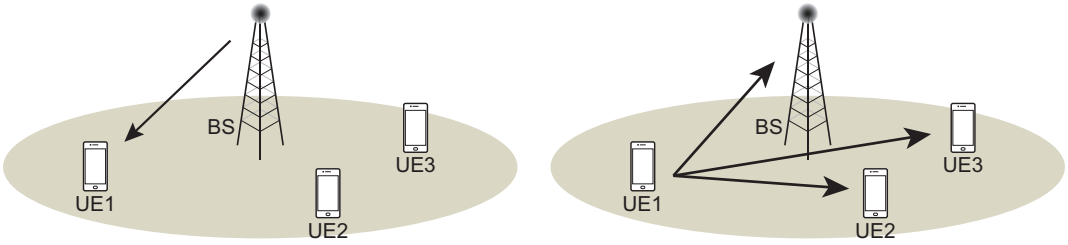

(a) Request from BS

(b) Sounding reference signal from UE1

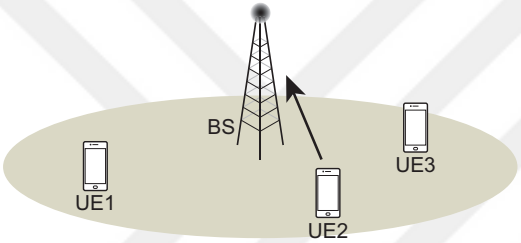

(c) Feedback from UE2

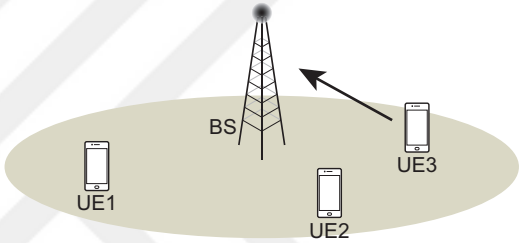

(d) Feedback from UE3

Figure 5.1: Measurement scheme

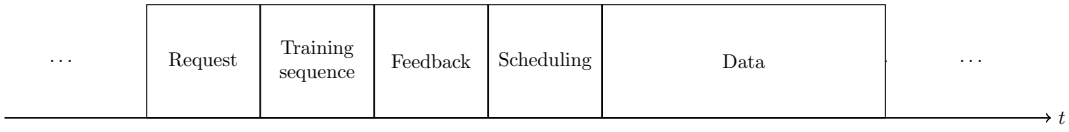

Figure 5.2: Generic timing scheme

are made they can be propagated and executed as usual. Some of the design parameters for this model are as follows:

Learning sequence is executed periodically during predetermined time slots and it can use reference signals that is used to measure UE-to-BS channel state. Time delay to next learning sequence is T_s.

A periodic uplink reference signal can be transmitted as frequent as 2 ms [29]. However not only such a small value would increase total overhead rate significantly but also considering practical mobility requirements, it would be wasteful to collect relatively large amount of data with low expected utility increase per slot. Therefore we choose $T_s = 10$ ms as inter learning sequence time. For the

We assume every node participates in feedback phase and complete information of their respective measurements are available at the scheduler.

The process described above is generated for $m;\ m \in \{1, \ldots, N\}$ different instances at a given sequence. This number influences efficiency of learning process and we assume m is fixed during a simulation.

The resulting overhead for sequential learning is calculated similar to full information case. We presume reference signal request and scheduling signals for our problem does not incur additional overhead as they are available and in use. This scheme uses m nodes as reference points for measurement, thus $m \times k_{\text{rs}}$ bits are reserved in UL and DL resources. Feedback process requires $m\,(N-1)\,k_{\text{fb}}$ bits are assigned in UL resources, and if channel reciprocity is assumed, selected nodes do not need to transmit same parameters so this overhead is reduced to $[m\,(N-1) - m\,(m-1)\,/2]\,k_{\text{fb}}$.

For the illustration purposes let each reference signal take one subframe $k_{\text{rs}} = 7$ and each feedback symbol take four bits $k_{\text{fb}} = 4$, then for 100 UE and $T_s = 10\,\text{ms}$ we can calculate overhead in kilobits per second and ratio of improvement over complete information case in terms of action size as given in Table 5.1.

Table 5.1: Overhead calculation for learning sequence

Action	Overhead [kb/s]	Improvement
$m = 100$	2118.6	-
$m = 2$	80.2	96.2%
$m = 4$	158.8	92.5%
$m = 8$	311.2	85.3%
$m = 10$	385.0	81.8%

These calculations show that limiting m lead to significant overhead reduction, but the resulting loss of channel state information can also degrade performance. Here we formulate the learning problem. Action $a(t)$ is the set of m nodes to initiate learning sequence by transmitting reference signals. The sequential process of inter-user channel measurement is to update the information used for allocation with the information obtained from the learning sequence sequentially. We would like to select a path of users equivalently a set of actions $a(0), \ldots, a(t)$ to

minimize the difference between the actual achievable capacity $R(t)$ using full CSI and capacity obtained with available information.

Let $\Delta r\left(a,t\right)=R\left(t\right)-r\left(a,t\right)$ select i,j such that

$$\arg\min_{a}\left(\Delta r\left(i,t\right)\right)$$

Number of possible actions prior to a given learning sequence is $\binom{N}{m}$, however to evaluate a particular action in terms of aggregate capacity it is required to know prior actions and time instances when they are executed to reconstruct pairing metric. Note that each previous action can also happen in $\binom{N}{m}$ different ways. In addition for an arbitrary policy, it is not clear how many previous actions should be considered. A policy that avoids selecting a partition of users after a certain time is an example where previous actions are unbounded as time goes to infinity. Due to these two properties, a value function can grow exponentially and reach unmanageable sizes even for sparse networks.

Transition function which represents change in node parameters due to mobility and shadowing are stochastic and not necessarily stationary processes. Therefore it is rather difficult to generate a structured approach due to extensive state and action space and obscurity of transition functions. We present deterministic and stochastic algorithms to solve this problem in the next section.

5.2 Learning Algorithms

Since modeling and optimizing the learning process in action-reward framework presents a large complexity, we take a heuristic approach. We learn the environment using Round-Robin, Uniform Weighted Random, Nonuniform Weighted Random algorithms. Algorithms are centralized and they are run in conjunction with a scheduler and they determine a set of nodes to be measured for the following learning sequence. Towards the solution of scheduling problem under mobility, we utilize LAPJV algorithm for its efficiency considering the number of users.

5.2.1 Round-Robin

Round-robin is a deterministic method which allocates an equal amount of learning opportunity to each node. At every sequence round-robin algorithm sets an action of m nodes with consecutive indices:

$$a\,(t) = \{i, i+1, \ldots, i+m\} \tag{5.1}$$

Time between two measurements of any node is upper bounded by $\lceil \frac{N}{m} \rceil$.

5.2.2 Uniform Weighted Random

Action $a\,(t)$ is selected among the full set of nodes equally likely.

5.2.3 Nonuniform Weighted Random

This stochastic method uses a weight vector W to generate a probability mass function which is then used to randomly select action of size m. At the beginning of full-duplex activation phase, we assume no information is available about the network topology, hence the weight vector is initialized to equally likely weights.

Once the vector containing inter UE interference is received for all m nodes, each row $i \in a(t)$ is inspected column by column for path loss smaller then threshold η. If such an entry is found in column j we duplicate the transposed vector to row j to improve pairing algorithm by making the assumption nodes that are close to each other have similar interference vectors. We then factor out weight of estimated node by β; $0 \leq \beta < 1$ to reduce the probability that this node is selected for next sequences.

This procedure by itself inherently introduces error to inter-user interference matrix G and it will influence pairing performance and it will delay measurement from estimated node. To constraint redundant we use two conditions. If there

are unknown elements, we update them selectively, otherwise we use a tighter threshold value $\eta\star$ to determine nearby nodes and to prevent loops we ensure previous value is changed at least five percent.

Once update procedure is complete, we use a parameter $\alpha,\ 0 \leq \alpha < 1$ to factor weight of previously selected users $a(t)$, to reduce their probability further and redistribute the weight they have lost to other users to satisfy probability axiom $\sum_{i=1}^{N} W_i = 1$.

Pseudo-algorithm that runs at every learning sequence is presented in Algorithm 1.

Algorithm 1 Weighted random algorithm

initialize $W \leftarrow \{1/N\}$
$nodes \leftarrow \{1, 2, \ldots, N\}$
$E \leftarrow \emptyset$ {set of estimated nodes}
$a \leftarrow$ select m random nodes from distribution W
Obtain g from learning sequence with a
if G has unknown elements **then**
  for all $i \in a$ **do**
    $V \leftarrow$ nodes with less than η loss to i
    for all $j \in V$ **do**
      fill empty elements of $g_j \leftarrow g_i$
      $E \cup j$
    end for
  end for
else
  for all $i \in a$ **do**
    $V \leftarrow$ nodes with less than $\eta\star$ loss to i
    for all $j \in V$ **do**
      if $g_j i$ and $g_i j$ differ **then**
        $g_j \leftarrow g_i$
        $E \cup j$
      end if
    end for
  end for
end if
for all $j \in E$ **do**
  $W \leftarrow W + W_j(1 - \beta)/(N - 1)$
  $W_j \leftarrow \beta W_j$
end for
for all $i \in a$ **do**
  $W \leftarrow W + W_i(1 - \alpha)/(N - 1)$
  $W_i \leftarrow \alpha W_i$
end for
pairs $\leftarrow$ matching(g)
schedule pairs

5.3 Numerical Results

In this section, we will present the simulation environment and evaluate algorithms under mobility.

5.3.1 Simulation Environment

Modifications are made to simulation environment in Chapter 3 as we incorporate user mobility. In order to investigate the effect clearly we extend the cell size and number of users to alleviate excessive interruption to node movement due to constrained space.

Simulation parameters are configured based on the scenario 2 of 3GPP specification [26] are given in Table 5.2. As in Chapter 3, we assume full buffers with heavy traffic in a single cell environment.

We evaluate two test cases to examine performance of sequential algorithms. The first setup covers the initial phase when the scheduler starts with no prior inter node interference information. Second setup is initialized with ideal user pairing configuration for all algorithms and after 10 ms mobility parameters are perturbed. At this time instance, users stop momentarily, select a new direction or waypoint and a new speed value according to new parameter set.

In order to illustrate relative performance with respect to channel state information knowledge we provide two endpoints:

- Random pairing performs user pairing without the knowledge of channel parameters and represents worst case with best possible overhead performance
- Ideal pairing runs the learning algorithm with N nodes to accumulate full information thus it is an indicator of best possible pairing performance for the given time instance but it also requires maximum amount of overhead

Table 5.2: Simulation Parameters

Parameter	Value
Cell radius	100 m
Initial UE Placement	Uniformly random
Maximum Pico TX power	24 dBm
Maximum UE TX power	23 dBm
Thermal noise density	-174 dBm/Hz
BS-UE Path loss model	$\mathrm{PL}_{\mathrm{LOS}}(R) = 103.8 + 20.9\log_{10}(R)$ $\mathrm{PL}_{\mathrm{NLOS}}(R) = 145.4 + 37.5\log_{10}(R)$
LOS probability	$0.5 - \min(0.5, 5\exp(-0.156/R))$ $+ \min(0.5, 5\exp(-R/0.03))$
UE-UE Path loss model	$R \leq 50m$;PL $= 98.45 + 20\log_{10}(R)$ $R > 50m$;PL $= 175.78 + 40\log_{10}(R)$
Noise figure	9 dB (UE) 13 dB (BS)
Shadowing std deviation BS and UE	3dB (LOS) 4dB (NLOS)

Visualization of results contain time domain data which appears noisy due to high frequency fluctuations. In order to make plots more coherent, we smooth out data using locally weighted polynomial regression (LOWESS) with first degree polynomial and moving window of 10 ms along time axis.

5.3.2 Mobility

In order to assess the learning performance, we introduce user mobility to achieve time variant parameters for pairing. In the following subsections we summarize two of the mobility models that we have used. Mobility data is generated using ns3 modules and then processed with main program code.

5.3.2.1 Random Walk Mobility Model

The properties of this model are as follows according to [30]. At each slot a uniformly distributed direction $\theta_i(t) \in [0, 2\pi]$ and a uniformly distributed speed

$v_i(t) \in [v_{min}, v_{max}]$ is selected for each node i. The process is memoryless so $\theta_i(t)$ and $v_i(t)$ are independent from past and previous values. Whenever a node arrives at the cell edge, the direction $\theta_i(t)$ is updated as $\theta_i(t) = \pi - \theta_i(t)$ so that the node stays inside the cell.

5.3.2.2 Random Waypoint Mobility Model

Random waypoint mobility model consists of selects a destination point uniformly random inside cell and starts moving to this waypoint with uniformly distributed speed $v_i(t) \in [v_{min}, v_{max}]$. Once node reaches its destination, it selects a time value from uniform distribution $[p_{min}, p_{max}]$, and waits for that duration prior to selecting its new waypoint.

In contrast to random walk mobility model where displacement between two time instances is quite limited due to Brownian motion, random waypoint model can introduce continuous movements that can span long distances across the cell.

5.3.3 Results

For the following simulations we use random waypoint mobility model. We use η, $\eta\star$ equivalent to 10m and 5m distances respectively, and set $\alpha = 0.01$, $\beta = 0.3$.

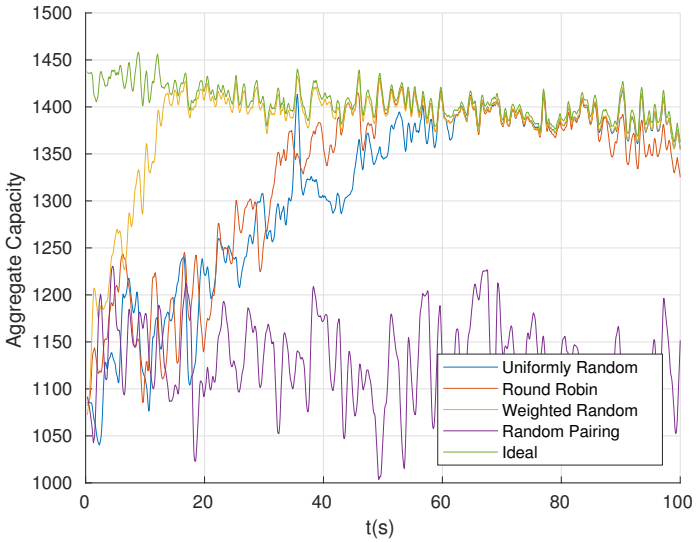

Figure 5.3: Random walk, vmax=10m/s, m=1

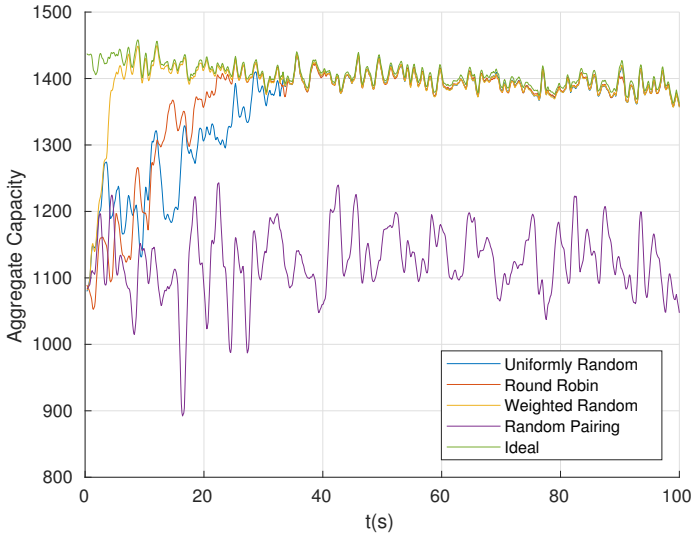

Figure 5.4: Random walk, vmax=10m/s, m=2

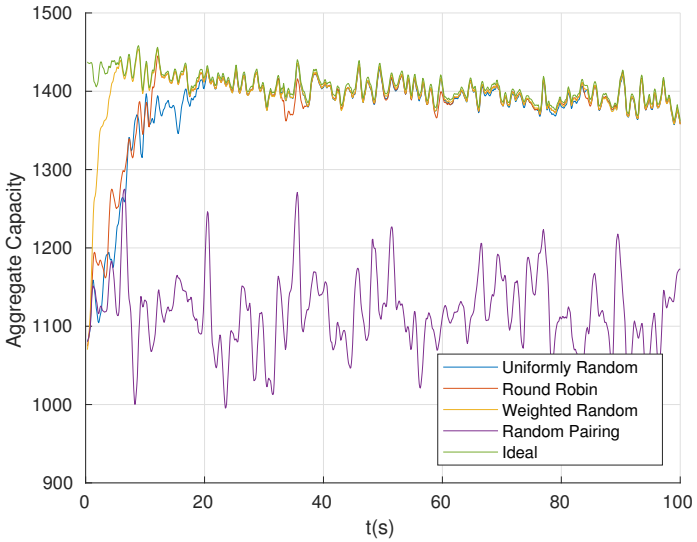

Figure 5.5: Random walk, vmax=10m/s, m=4

For the cases with action sizes 1,2,4 nonuniform weighted random algorithm converges approximately 60% faster than round robin algorithm. Uniformly random algorithm performs the worst, but it can surpass round robin for certain periods of time. These experiments often contain transient effects such as the spike uniformly random weighted algorithm has at 34s in Figure 5.3. Since every inter-user interference vector at an arbitrary time have a different contribution to pairing process, it is possible that such a spike can persistently improve subsequent performance. However in this occurrence utility matrix does not contain sufficient information, so it can be inferred that the pairing is influenced randomly.

Here, maximum speed parameter of mobility model is doubled to 20m/s.

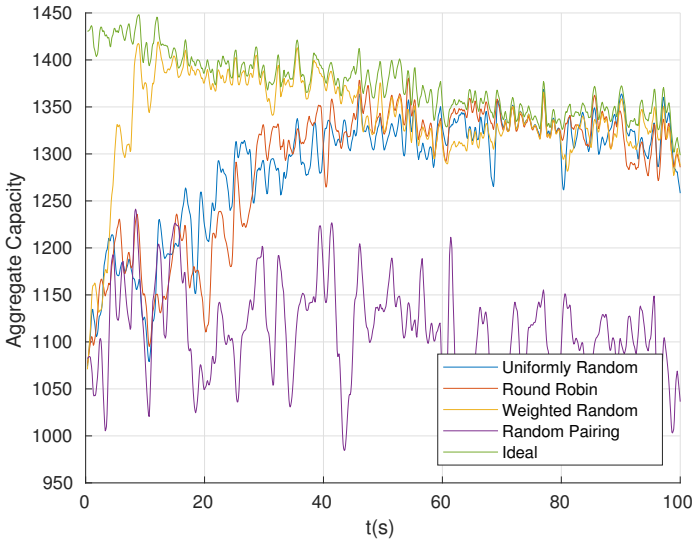

Figure 5.6: Random walk, vmax=20m/s, m=1

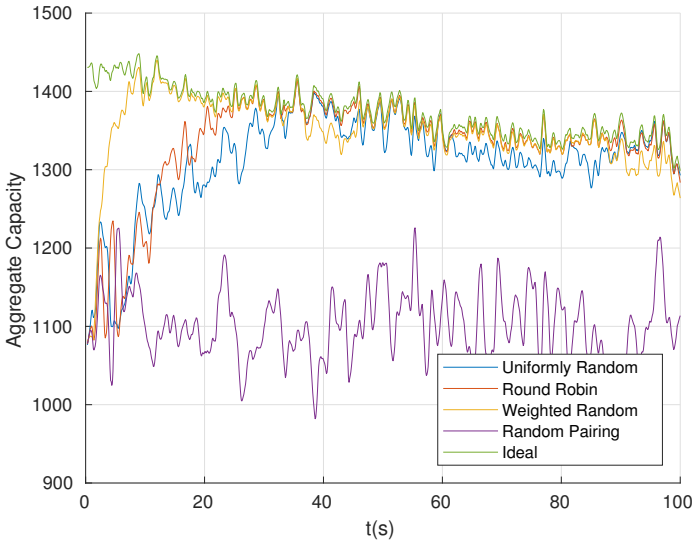

Figure 5.7: Random walk, vmax=20m/s, m=2

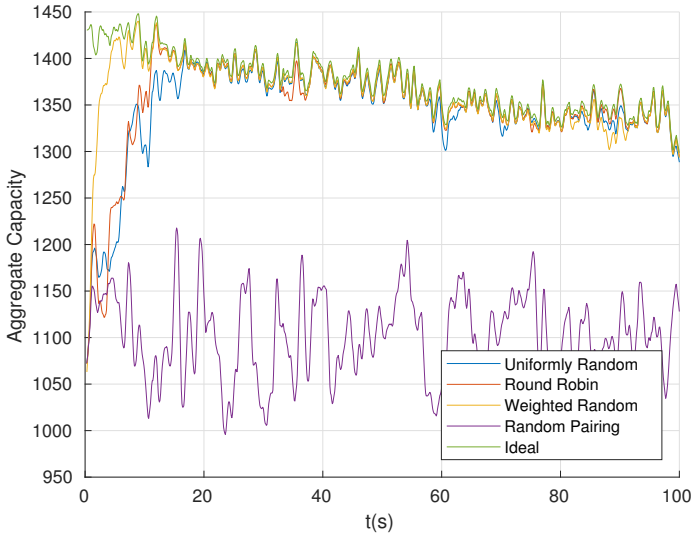

Figure 5.8: Random walk, vmax=20m/s, m=4

In Figure 5.6 due to simultaneously changing network parameters, achieving near optimal aggregate capacity takes more time, since learned parameters not only become obsolete but also influence pairing algorithm. Nonuniform weighted algorithm is relatively faster than the other two compared to vmax=10m/s case. Uniformly random selection has difficulty obtaining optimal performance in Figure 5.7.

From these experiments, we make the observation that round robin algorithm reaches optimum performance after $N/2$ sequences per measurement node. In other words, we expect convergence at $N/2m$ measurement. The effect of action size can be abstracted with this notion and failure in this pattern might indicate selected action size is too low to track the environment.

For the following simulations, we use random waypoint mobility model. Note that this model has a slightly different steady state user distribution than uniform [30]. To reject transient sum capacity changes we dropout 10^3 seconds of initial movement to better approximate steady state positioning.

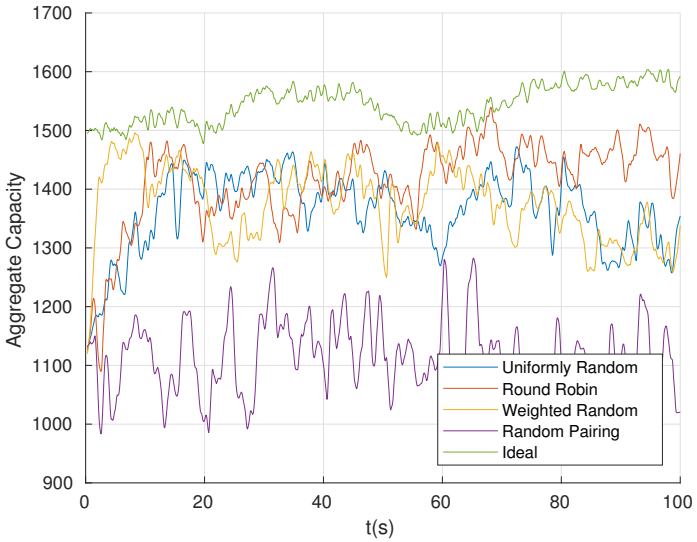

Figure 5.9: Random waypoint, vmax=10m/s, m=4

In Figure 5.9, the action size of four is not sufficient to track user mobility for all algorithms. Nonuniform weighted algorithm still rapidly converges close to optimum solution but drops back to the level of others. We note that although average user speeds are consistent between random walk and random waypoint models, displacement of a user in the latter model during a period of time is greater. Therefore it can be stated that random waypoint model is more challenging in context of tracking link geometries between users.

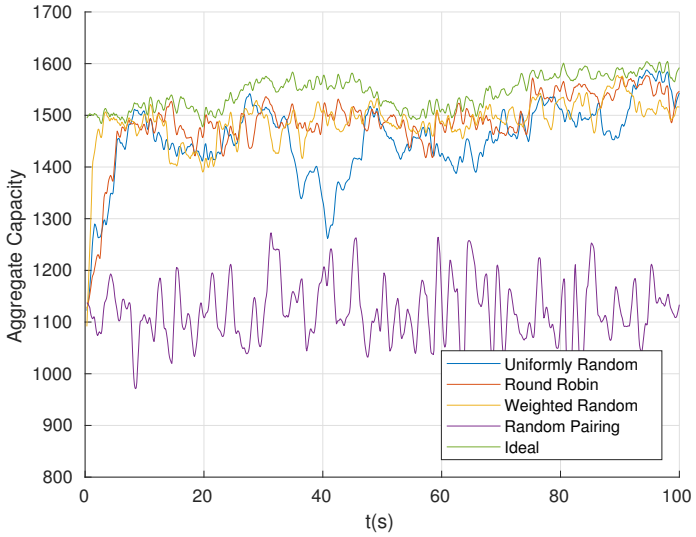

Figure 5.10: Random waypoint, vmax=10m/s, m=8

For the following simulations, we setup the environment as before but introduce perturbation to user mobility at $t = 10$. Initial conditions for user pairing are taken from the steady state values of previous experiments. Therefore result simulation starts with performance of optimum pairing. As soon as perturbation occurs at designated time, users stop and change their direction and speed, rendering the accumulated information at scheduler obsolete. In order to isolate the effect of recovery, we prefer a scenario with less mobility activity and low number of measurement nodes.

In Figure 5.11, initially random walk mobility with vmax=10m/s is assumed and perturbation event doubles maximum speed to vmax=20m/s.

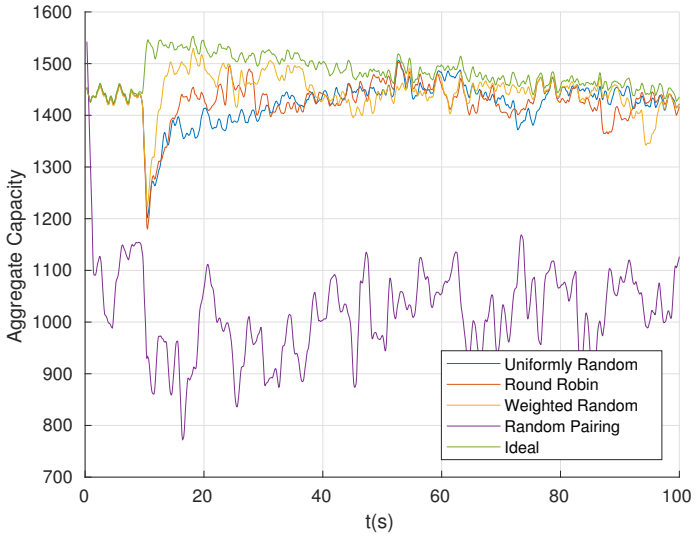

Figure 5.11: Random walk with perturbation, m=2

Similar to initial phase experiments, weighted algorithm with tuned parameters under perturbation condition can converge faster than other algorithms. However we observe that estimation inter-user interference values have an adverse effect. Depending on the threshold to select nearby nodes, a trade-off between settling time and tracking error is present. The simulation provided in 5.11 features a threshold equivalent of 10m distance and has notable tracking error. Further increasing the threshold results in oscillations. A conservative value on the other hand is slower to converge.

In Figure 5.12, we consider inverted case where simulation starts with random walk mobility with vmax=20m/s and perturbation event relaxes maximum speed to vmax=10m/s.

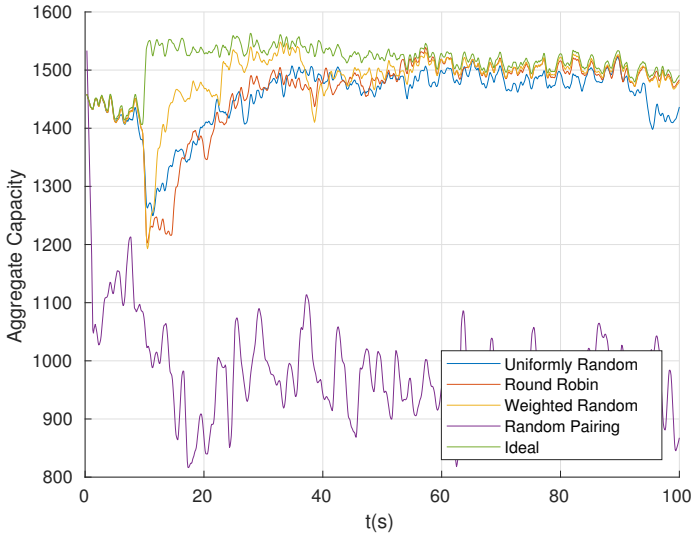

Figure 5.12: Random walk with perturbation, m=2

We observe that the pattern for average sum capacity is consistent with previous perturbation case. As expected tracking error of weighted random algorithm is decreased due to constrained user mobility after perturbation. Reducing distance threshold in this context could only superficially contribute to steady state error. Therefore it can be concluded that the value of threshold should be selected assertively with consideration of risk induced in worse case scenarios for stability.

Chapter 6

Conclusions

In this thesis, user pairing and grouping methods is studied in single cell wireless network with full-duplex base station and half-duplex mobile stations.

For the pairing problem, it is shown that as the number of users increase, for the uniform user placement case, the pairing algorithm gradually performs better. This is due to the fact that it is possible to locate more prospective pairs which consist of users imposing lower inter-user interference figure to each other. On the other hand, analytic solution for random pairing suggests an important conclusion about user placement. As it is shown, under random geometry and random pairing conditions there exists pairs with capacities close to the ones that are obtained with linear integer programming solution. The number of such pairs hence the weight of their presence relative to network distribution is a direct consequence of using uniformly random distribution. As a result, topological limitations for our scenario can be used as an advantage in certain geographical contexts.

The learning based approach for obtaining inter-user interference parameters is evaluated. The initial estimation procedure for the missing elements significantly reduce the time delay to reach optimal pairing algorithm with full information. It is observed that random waypoint model due to its large influence in link

geometries between nodes causes larger perturbation to aggregate capacity for the same maximum velocity parameter as the random walk model. It is also observed that the tracking error for large mobility activity for this mobility model is considerably larger and can lead to failure.

In future works, a control system can be implemented to tune the action and threshold parameters to improve robustness against fluctuations in network parameters while retaining rapid convergence features to further improve efficiency in networks with mobility.

Bibliography

[1] Cisco, "Cisco Visual Networking Index: Global Mobile Data Traffic Forecast Update, 2016–2021," tech. rep., 2017.

[2] ITU, "IMT Vision – Framework and overall objectives of the future development of IMT for 2020 and beyond," vol. 0, p. 21, 2015.

[3] A. Molisch, *Wireless Communications*. Wiley-IEEE Press, 2005.

[4] D. Kim, H. Lee, and D. Hong, "A survey of in-band full-duplex transmission: From the perspective of phy and mac layers," *IEEE Communications Surveys Tutorials*, vol. 17, pp. 2017–2046, Fourthquarter 2015.

[5] A. Sabharwal, P. Schniter, D. Guo, D. W. Bliss, S. Rangarajan, and R. Wichman, "In-band full-duplex wireless: Challenges and opportunities," *IEEE Journal on Selected Areas in Communications*, vol. 32, no. 9, pp. 1637–1652, 2014.

[6] J. I. Choi, M. Jain, K. Srinivasan, P. Levis, and S. Katti, "Achieving single channel, full duplex wireless communication," in *Proceedings of the Sixteenth Annual International Conference on Mobile Computing and Networking*, MobiCom '10, (New York, NY, USA), pp. 1–12, ACM, 2010.

[7] M. Liu, Y. Mao, S. Leng, X. Huang, and Q. Zhao, "Traffic-aware resource allocation for full duplex wireless networks," in *2016 IEEE/CIC International Conference on Communications in China, ICCC 2016*, 2016.

[8] M. Jain, J. I. Choi, T. Kim, D. Bharadia, S. Seth, K. Srinivasan, P. Levis, S. Katti, and P. Sinha, "Practical, real-time, full duplex wireless," *Proceedings of the 17th annual international conference on Mobile computing and networking (MobiCom '11)*, p. 301, 2011.

[9] D. Bharadia, E. McMilin, and S. Katti, "Full Duplex Radios," *SIGCOMM Comput. Commun. Rev.*, vol. 43, pp. 375–386, aug 2013.

[10] M. Duarte, A. Sabharwal, V. Aggarwal, R. Jana, K. K. Ramakrishnan, C. W. Rice, and N. K. Shankaranarayanan, "Design and characterization of a full-duplex multiantenna system for wifi networks," *IEEE Transactions on Vehicular Technology*, vol. 63, no. 3, pp. 1160–1177, 2014.

[11] S. Goyal, P. Liu, S. Panwar, R. A. DiFazio, R. Yang, J. Li, and E. Bala, "Improving small cell capacity with common-carrier full duplex radios," in *2014 IEEE International Conference on Communications (ICC)*, pp. 4987–4993, June 2014.

[12] R. Li, Y. Chen, G. Y. Li, and G. Liu, "Full-Duplex Cellular Networks: It Works!," pp. 1–15, 2016.

[13] X. Xie and X. Zhang, "Does full-duplex double the capacity of wireless networks?," in *IEEE INFOCOM 2014 - IEEE Conference on Computer Communications*, pp. 253–261, April 2014.

[14] T. Le-Ngoc and A. Masmoudi, *Full-Duplex Wireless Communications Systems*. Wireless Networks, Cham: Springer International Publishing, 2017.

[15] M. Heino, D. Korpi, T. Huusari, E. Antonio-Rodr??guez, S. Venkatasubramanian, T. Riihonen, L. Anttila, C. Icheln, K. Haneda, R. Wichman, and M. Valkama, "Recent advances in antenna design and interference cancellation algorithms for in-band full duplex relays," *IEEE Communications Magazine*, vol. 53, no. 5, pp. 91–101, 2015.

[16] M. Al-Imari, M. Ghoraishi, P. Xiao, and R. Tafazolli, "Game theory based radio resource allocation for full-duplex systems," in *2015 IEEE 81st Vehicular Technology Conference (VTC Spring)*, pp. 1–5, May 2015.

[17] J. Bae, E. Park, K. Chang, H. Ju, and Y. Han, "In-band full-duplex system throughput analysis for wi-fi outdoor network," in *Vehicular Technology Conference (VTC Fall), 2015 IEEE 82nd*, pp. 1–5, Sept 2015.

[18] B. Di, S. Bayat, L. Song, and Y. Li, "Radio resource allocation for full-duplex OFDMA networks using matching theory," *2014 IEEE Conference on Computer Communications Workshops (INFOCOM WKSHPS)*, pp. 197–198, 2014.

[19] M. Duarte, A. Feki, and S. Valentin, "Inter-user interference coordination in full-duplex systems based on geographical context information," in *2016 IEEE International Conference on Communications (ICC)*, pp. 1–7, May 2016.

[20] C. Nam, C. Joo, S. G. Yoon, and S. Bahk, "Resource allocation in full-duplex OFDMA networks: Approaches for full and limited CSIs," *Journal of Communications and Networks*, vol. 18, no. 6, pp. 913–925, 2016.

[21] R. Jonker and A. Volgenant, "A shortest augmenting path algorithm for dense and sparse linear assignment problems," *Computing*, vol. 38, pp. 325–340, Dec 1987.

[22] R. Burkard, M. Dell'Amico, and S. Martello, *Assignment Problems*. Society for Industrial and Applied Mathematics, 2012.

[23] D. Gusfield and R. W. Irving, *The stable marriage problem : structure and algorithms*. Foundations of computing, Cambridge, Mass. : MIT Press, c1989., 1989.

[24] D. Knuth, *Stable Marriage and Its Relation to Other Combinatorial Problems: An Introduction to the Mathematical Analysis of Algorithms*. CRM proceedings & lecture notes, American Mathematical Society, 1997.

[25] F. P. Kelly, A. K. Maulloo, and D. K. H. Tan, "Rate control for communication networks: shadow prices, proportional fairness and stability," *Journal of the Operational Research Society*, vol. 49, pp. 237–252, Mar 1998.

[26] "Further enhancements to lte time division duplex (tdd) for downlink-uplink (dl-ul) interference management and traffic adaptation," TR 36.828 11.0.0, 3GPP, June 2012.

[27] D. Moltchanov, "Distance distributions in random networks," *Ad Hoc Networks*, vol. 10, no. 6, pp. 1146–1166, 2012.

[28] H. Solomon, *Geometric Probability*. CBMS-NSF Regional Conference Series in Applied Mathematics, Society for Industrial and Applied Mathematics, 1978.

[29] E. Dahlman, S. Parkvall, and J. Skold, *4G: LTE/LTE-Advanced for Mobile Broadband*. Elsevier Science, 2013.

[30] R. Roy, *Handbook of Mobile Ad Hoc Networks for Mobility Models*. New York: Springer, 2011.

[31] S. Goyal, P. Liu, and S. S. Panwar, "User selection and power allocation in full duplex multi-cell networks," *IEEE Transactions on Vehicular Technology*, vol. PP, no. 99, pp. 1–1, 2016.